LUND UNIVERSITY

Microrheology of Concentrated Protein Solutions

Garting, Tommy

2019

Microrheology of Concentrated Protein Solutions

TOMMY GARTING | PHYSICAL CHEMISTRY | LUND UNIVERSITY

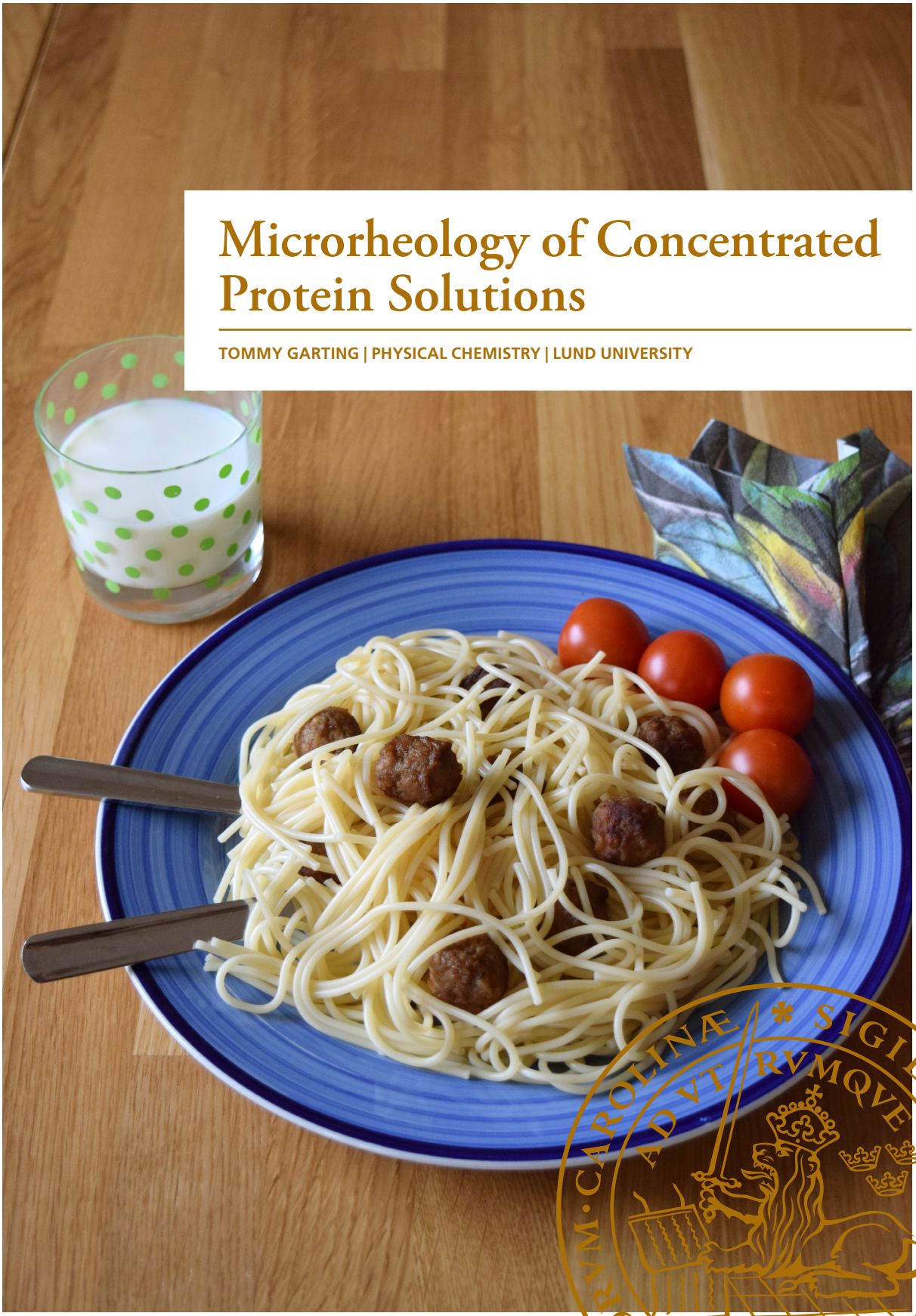

Microrheology of Concentrated Protein Solutions

Microrheology of Concentrated Protein Solutions

by Tommy Garting

LUND
UNIVERSITY

DOCTORAL DISSERTATION

by due permission of the Faculty of Science, Lund University, Sweden.
To be defended on Friday, the 22nd of February 2019 at 13:15 in Lecture hall B at the Department of Chemistry, Lund University.

Faculty opponent

Professor Frank Scheffold
University of Fribourg, Fribourg, Switzerland

Organization	Document name
LUND UNIVERSITY Department of Chemistry Box 124 SE–221 00 LUND Sweden	**DOCTORAL DISSERTATION** Date of disputation 2019-02-22 Sponsoring organization
Author(s) Tommy Garting	

Title and subtitle

Microrheology of Concentrated Protein Solutions:

Abstract

The behavior of concentrated protein solutions is of general high interest due to implications in, for example, biological systems and medical applications. It is necessary to investigate the rheological properties of such systems to understand how parameters, such as stability, are affected by the high concentrations. Unfortunately, studies are often hindered by the lack of sufficient quantities of the protein of interest. A collection of techniques have been suggested as a way to circumvent this issue by requiring much smaller sample volumes. These techniques are commonly collated by the term ”microrheology” and are based on observing the motion of tracer particles immersed in a sample.

This thesis describes the work of preparing tracer particles suitable for scattering- and microscopy-based microrheology of concentrated protein solutions. Different proteins were investigated using the aforementioned methods, including several present in the eye lens system which has a necessity of high protein concentrations to function optimally. Employing a secondary sample preparation step involving evaporation made it possible to reach into the arrested regime of close-packed proteins. Samples in this region are of high scientific interest but commonly difficult to produce and investigate.

Key words

Microrheology, Dynamic Light Scattering, Protein, Pegylation, Viscosity

Classification system and/or index terms (if any)

Supplementary bibliographical information	Language
	English
ISSN and key title	ISBN
	978-91-7422-624-9 (print) 978-91-7422-625-6 (pdf)
Recipient’s notes	Number of pages: 151 / Price
	Security classification

Microrheology of Concentrated Protein Solutions

by Tommy Garting

LUND
UNIVERSITY

A doctoral thesis at a university in Sweden takes either the form of a single, cohesive research study (monograph) or a summary of research papers (compilation thesis), which the doctoral student has written alone or together with one or several other author(s).

In the latter case the thesis consists of two parts. An introductory text puts the research work into context and summarizes the main points of the papers. Then, the research publications themselves are reproduced, together with a description of the individual contributions of the author. The research papers may either have been already published or are manuscripts at various stages (in press, submitted, or in draft).

Cover illustration front: Experiment in progress.

Faculty of Science, Department of Chemistry, Division of Physical Chemistry

ISBN: 978-91-7422-624-9 (print)
ISBN: 978-91-7422-625-6 (pdf)

Printed in Sweden by Media-Tryck, Lund University, Lund 2019

Media-Tryck is an environmentally certified and ISO 14001:2015 certified provider of printed material. Read more about our environmental work at www.mediatryck.lu.se

MADE IN SWEDEN

Till Alicia & Signe

TABLE OF CONTENTS

Acknowledgements

First and foremost, a huge thank you to my main supervisor Anna Stradner for believing in me and providing the opportunity to work on this interesting and challenging project. None of this would have been possible without your help and support. I can't thank you enough for letting me be a part of your research group.

I would like to thank my assistant supervisor Ulf Olsson, who also initially put me in contact with Anna thus making this adventure possible. I'm also very grateful for my previous assistant supervisors, Marc Obiols-Rabasa and Peter Schurtenberger, for all the discussions and for teaching me a lot about scattering methodology.

A very special thanks to my office/lab mates throughout the years: Saskia, Lucia, Najet, Nicholas, Jin-Suk, Felix and Alessandro who made work so much more enjoyable. A special shout-out to Saskia for teaching me everything on how to obtain and handle eye lens proteins, for better or worse I won't forget it. I also want to thank Nicholas for letting me work on his antibodies and Felix for providing Linux expertise as well as feedback on the thesis.

Maxime, I don't know where this project would have ended up without you, but it would definitely not have been in such a fun place #aac. I also want to thank Ricardo and Axel for the interesting side projects even though they didn't end up in this thesis.

I also want to acknowledge Lenke Horváth, Aurélien Crochet and Katharina Fromm at Fribourg University, without their help my trip to Switzerland would have been near impossible. I would like to thank Krister Holmgren for flipping through a powerpoint slide containing protein adsorption on pegylated surfaces, without it I don't know if I would have been able to make the particles work.

I have had the fortune of getting to know way too many people at Physical Chemistry to mention everyone, but rest assured that I'm grateful for the time I got to spend with all of you. A special thanks to Sanna, Marianna and Charlotte who welcomed me into the community back when I started, as well as to Stefanie and Vicky who tagged along to countless coffee-breaks.

There are several important people that were not directly involved in my research but without their help everything would have been exponentially more difficult. Thank you Helena, Maria, Peter and Chris for making everything run smoothly at the division. I also want to acknowledge the help Paula provided with formatting and printing this thesis.

Thank you to all the people that have contributed to the Latex-template on which this thesis is based upon. I'm also happy that I was not alone in this boat, but was able to share and learn ideas and tricks with Linda, Maxime and Jasper throughout these last months. The impromptu ventilation sessions, including walks, were definitely well needed.

Jag kan heller inte förringa betydelsen av söndagarnas filosofi-cirkel med Daniel, Tobias, Anders och Arvid för att bryta av veckornas arbete. Det var också väldigt fint att driva en arbetarpodd med dig Daniel, det är det ingen som gör nuförtiden.

Slutligen vill jag tacka min familj! Mina föräldrar och min bror som alltid hjälpt och stöttat mig. Kajsa, jag kan inte tänka mig en bättre livskamrat, tack för alla åren som har gått och till de som kommer framöver. Alicia och Signe som alltid lyckas förvandla dåliga dagar till de bästa av dagar.

Populärvetenskaplig Sammanfattning

Tack vare ett näst intill oändligt antal variationer så har proteiner blivit naturens standardlösning för diverse uppgifter och problem. I våra egna kroppar har vi en uppsjö av olika varianter där några är allmänt välkända, t.ex. hemoglobin i våra röda blodkroppar som transporterar runt syre och insulin vilket sänker vår blodsockernivå. Andra proteiner är mer okända men trots det lika viktiga, exempelvis haptoglobin vars uppgift är att rensa bort hemoglobin som kommit på avvägar, samt glukagon som höjer vår blodsockernivå vid behov.

Ett annat användningsområde för proteiner är i ögats lins som innehåller extremt höga proteinkoncentrationer, faktiskt de högsta som vi har i kroppen. Just i linsen har naturen utnyttjat att en proteinlösning bryter ljus; ju högre koncentration desto starkare brytning vilket i våra ögon bidrar till att fokusera inkommande ljus på näthinnan så att vi kan se klart och tydligt. En effekt av de höga koncentrationerna är att interaktioner mellan proteiner leder till ökad viskositet, d.v.s. hela systemet blir mer trögflytande. Det är en viktig egenskap eftersom linsen måste kunna ändra form för att vi ska kunna fokusera på endera långt eller nära håll.

Normalt sett innehåller celler, förutom proteiner, ett stort antal olika komponenter men cellerna i ögats lins gör sig av med i princip alla extra komponenter under fosterutvecklingen. Detta är nödvändigt för att linsen ska vara genomskinlig, vi kan exempelvis inte se igenom vår hud p.g.a. allt som sprider och absorberar ljus. Det här har dock nackdelen att förmågan till att skapa nya proteiner också försvinner, vilket innebär att de ögonlinsproteiner vi har när vi föds är de vi behöver använda under resten av livet. Proteinerna i ögonlinsen måste därför vara stabila under hela vår livslängd vilket är extra problematiskt vid höga proteinkoncentrationer.

Det finns en reell risk, särskilt vid höga koncentrationer, att proteiner klumpar ihop sig och faller ur lösning vilket orsakar okontrollerad ljusspridning. Ifall det sker i tillräcklig omfattning i ögats lins kommer den inte längre att vara fullt genomskinlig och synen blir därmed oskarp. Det här är orsaken till sjukdomen grå starr vilken behandlas genom att kirurgiskt byta ut linsen mot en konstgjord variant. För att försöka förhindra sådana problem finns det gott om speciella skyddsproteiner i ögats lins vars uppgift är att hålla de andra proteinerna stabila. En annan vanlig, men mindre dramatisk, åkomma är ålderssynthet som gör att vi får svårt att fokusera på saker nära oss, såsom texten i vår favoritbok. Det beror på att linsen blir mer trögflytande med åldern och inte längre kan ändra sin form lika effektivt, vilket ofta kan kompenseras genom användandet av läsglasögon men kan även behandlas kirurgiskt likt andra synkorrigeringsoperationer.

Det finns metoder, vilka gemensamt går under namnet reologi, som används för att studera just sådana materialförändringar som resulterar i exempelvis ändrad viskositet. Ett stort problem vid reologiska studier av proteinsystem, som det i ögats lins men även för vissa proteinbaserade mediciner, är att experimenten behöver utföras vid de höga koncentrationer som de normalt sett finns i för att ge tillförlitliga svar. Framställning av tillräckliga mängder protein för att nå höga koncentrationer är ofta ett dyrt och tidskrävande åtagande varför man gärna vill utnyttja tekniker som klarar av små mätvolymer.

En speciell kategori av reologiska tekniker som endast behöver små volymer är mikroreologi. De utmärker sig genom att man tillsätter små nano/mikrometer-partiklar i proverna och sedan studerar hur dessa rör sig för att på så sätt få fram information om provet som helhet. Det är exempelvis möjligt att bestämma viskositeten av ett prov utifrån hur partiklarnas spontana, slumpmässiga rörelser påverkas av olika proteinkoncentrationer. För att sådana mätningar ska vara tillförlitliga är det viktigt att de tillsatta partiklarna inte har några märkbara interaktioner med vare sig varandra eller proteinerna.

Den här avhandlingen beskriver forskning centrerat kring partiklar som är behandlade just för att inte interagera med sin omgivning. De har sedan använts för att undersöka olika proteiner, däribland några av de som finns i ögats lins, i mikroreologiska experiment baserade på ljusspridning och mikroskopi. En kombination av olika metoder möjliggjorde förberedandet av de höga proteinkoncentrationer som finns i ögats lins fast i mikrolitervolymer. Den här metodiken kan även användas för att studera andra system där man är intresserad av de höga koncentrationer då ett system har så pass hög viskositet att det inte längre kan beskrivas som ett flytande material.

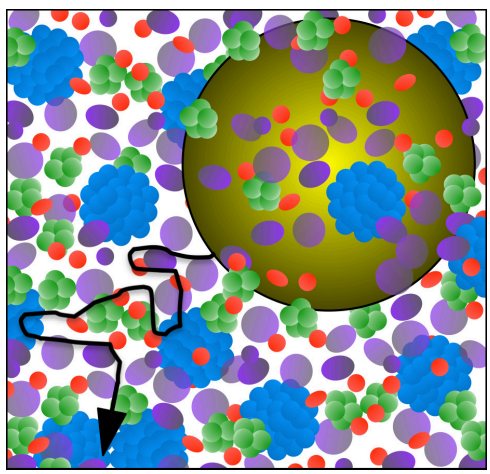

Illustrativ bild av mikroreologi publicerad som en grafisk representation till Paper I

List of Publications

This thesis is based on the following publications, referred to by their Roman numerals:

I **Optical Microrheology of Protein Solutions Using Tailored Nanoparticles**

T. Garting, A. Stradner
Small **2018**, 1801548

II **Synthesis and Application of PEGylated Tracer Particles for Measuring Protein Solution Viscosities Using Dynamic Light Scattering-Based Microrheology**

T. Garting, A. Stradner
Submitted to Colloids and Surfaces B: Biointerfaces - Protocols Article

III **Experimental Evidence for a Cluster Glass Transition in Concentrated Lysozyme Solutions**

[M. J. Bergman, **T. Garting**], P. Schurtenberger, A. Stradner
Submitted to Journal of Physical Chemistry B - Article

IV **Dynamical Arrest for Globular Proteins with Patchy Attractions**

[**T. Garting**, M. J. Bergman], P. Schurtenberger, A. Stradner
Manuscript

Abbreviations

BSA Bovine serum albumin 24, 39

CLSM Confocal laser scanning microscope 31, 40, 41

DLS Dynamic light scattering 19, 21, 24, 25, 28, 29, 31, 36, 37, 39–41, 44, 45, 47

DTT DL-Dithiothreitol 8

DWS Diffusing wave spectroscopy 24

EDC N-(3-dimethylaminopropyl)-N'-ethylcarbodiimide 27

EDTA Disodium ethylenediaminetetraacetate dihydrate 8

Hepes 4-(2-hydroxyethyl)-1-piperazineethanesulfonic acid 7

IEX Ion exchange 9

kDa kilo Dalton, molecular weight: 1 Da = 1 g/mol 4–7, 9, 27, 34, 36, 37

mAB Monoclonal antibody 7, 33–35

MES 2-(N-morpholino)ethanesulfonic acid 27

MPT Multiple particle tracking 31, 41, 42, 44, 45

MQ-H_2O Water purified with Milli-Q, 0.22 µm, system 7, 27, 29

MSD Mean squared displacement 25, 28, 29, 41, 42

PDI Polydispersity index 21

PEG Polyethylene glycol 27, 34, 36–38, 48

rcp Random close packing 13

SALR Short-range attraction and long-range repulsion 4, 16, 39

SEC Size exclusion chromatography 8

SLS Static light scattering 19, 21

Important Notations

A	Hamaker constant. 26
α	Eye lens protein, α-crystallin. 5, 8, 9, 33, 38, 39, 42–44
β	Eye lens protein, β-crystallin. 5, 6, 44
β_H	Subgroup of β-crystallin with high molecular weight. 6, 33, 43
D	Diffusion coefficient. 20, 21
d	Distance between two particle surfaces. 26
η	Viscosity. 21, 28
$[\eta]$	Intrinsic viscosity. 13–15, 43
η_r	Relative viscosity. 13–15, 28
$g^{(1)}$	Field autocorrelation function. 19, 20
$g^{(2)}$	Intensity autocorrelation function. 19, 20
γ	Eye lens protein, γ-crystallin. 5, 6, 8, 9, 44
γ_B	Subgroup of γ-crystallin, also called γ_{II}. 6, 7, 9, 33, 43–45, 47
μ_x	Cumulant coefficient of x:th order. 20
ν	Coefficient for fitting an attractive system. 15, 45
Φ	Volume fraction. 10, 13
Φ_c	Critical volume fraction. 44, 45
Φ_{eff}	Effective volume fraction. 14, 40
Φ_{max}	Volume fraction of the arrest transition. 13–15, 39, 40, 43, 45
$\vec{q}$	Scattering vector. 18, 19
R_H	Hydrodynamic radius. 21
T_c	Critical temperature. 44, 46
θ	Scattering angle. 18

Det har jag aldrig provat förut, så det klarar jag säkert.
— Pippi Långstrump

CHAPTER 1
INTRODUCTION

The inner workings of the eye lens is seldom talked about even though it is a crucial component for allowing us to perceive our environment. The ability of the lens to focus images on the retina relies, among other factors, on very high protein concentrations, typically several hundred mg/ml with the exact concentrations depending on the observed species. The fact that the lens can remain stable over decades at these concentrations is nothing short of wondrous, especially considering that the machinery to produce more protein is expelled during infancy in favor of light transmission. However, sometimes the lens will fail, commonly in association with illnesses such as cataract and presbyopia. Although external causes may affect the onset of such conditions they are naturally often just age related. (*Chapter 2*)

In a condition such as presbyopia, the ability of the lens to reshape, in response to muscles acting on it, is gradually lost due to enhanced stiffness of the lens. A possible way to study such a macroscopic transformation of a system would be to investigate the accompanying change in viscosity, since this is a direct measure of a systems ability to rearrange in response to external forces. An interesting aspect of viscosity is that for many systems it is only slightly affected by increasing concentrations, until a certain point. Once the system becomes rather close packed, rearrangement becomes exponentially more difficult and the viscosity vastly increases by several orders of magnitude, often over a relatively minor concentration range. (*Chapter 3*)

To properly study this type of arrest transition one ought to study the system at the corresponding elevated concentrations. This is especially true, but not exclusive, for the proteins in the eye-lens where the native concentrations are already quite close to these levels. This is by no means an easy feat as the availability is low and the procedure for obtaining the protein is rather involved and time consuming. A group of techniques, commonly denoted microrheology, has been proposed to alleviate this concern as they

only require small sample volumes. This commonly involves tracking the mobility of immersed tracer particles using different scattering and/or microscopy techniques. (*Chapter 4 and 5*)

The work presented in this thesis was initially focused on preparing suitable tracer particles for use with protein based systems. Once appropriate particles had been identified, these were then utilized to characterize various protein systems including several present in the eye-lens. Reaching concentrations at and beyond the arrest transition proved difficult but was finally achieved on a scale suitable for microscopy-based microrheology. (*Chapter 6*)

He then deliberately turned the focus of a protein depolarizer on himself and fell instantly and painlessly dead.
— Isaac Asimov

CHAPTER 2

PROTEINS

Contents

Due to the high versatility of proteins they are utilized by living entities on our planet for vastly different tasks within their bodies, as well as outside for certain species such as venomous snakes. These tasks can range from catalytic with enzymes[1] and defensive capabilities of antibodies[2] to structural components with e.g. actin[3]. The function of proteins is not only determined by their chemical composition but also from their three-dimensional structure. As such, they are sensitive to perturbations that infer structural disorder which may lead to serious diseases in the host body, such as Parkinson's, Alzheimer's and Huntington's disease.[4] A special class of proteins, commonly called chaperone or heat-shock proteins, are tasked with preventing these types of structural changes by physically restricting other proteins from losing their native shape.[5] Protein systems are thus highly interesting research objects both from a biological point of view but also as treatment possibilities for various diseases e.g. with antibody based medicine.

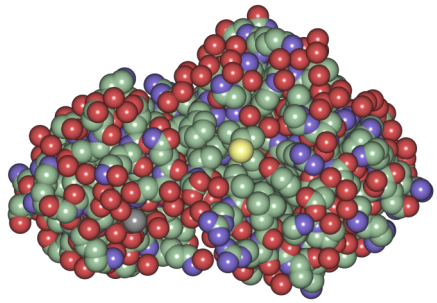

Figure 2.1: Atomic representation of lysozyme. [15]

2.1 Protein Systems

2.1.1 Lysozyme

Lysozyme, shown in figure 2.1, is a small globular protein, 14.4 kDa and dimensions $4.5 \times 3 \times 3$ nm,[6] and is a major component of the white in hen egg from where it is also produced. Its native use in the egg white is of enzymatic nature as a protection against potential bacterial infections during prenatal development by breaking down the cell membrane of bacteria, i.e. lysis, which is also where the name lysozyme originates.[7] Due to its abundance, resulting in a relatively low cost, and ease of forming crystals it is commonly used for studying protein crystallization. Despite being a monomeric protein it displays a complex phase behaviour due to its inherent protein interactions. Away from the isoelectric point and at low ionic strength, these consist of repulsive long-range electrostatic and attractive short-range van-der-waals like interactions, commonly abbreviated as SALR for Short-range Attraction and Long-range Repulsion. This was reported in 2004 where lysozyme was shown to form equilibrium clusters due to the interplay between these forces at buffer conditions with low ionic strength where the electrostatic repulsion was not significantly screened.[8] The structure and spatial distribution of proteins in a solution is of high interest in, for example, biological systems where it may be a sign of, or lead to, diseases in the organism.[9,10] Lysozyme has thus been heavily investigated in the past years to further understand the behavior of this type of system, especially interesting is the behavior at higher concentrations where a cluster glass would be expected. There are some discrepancies of the system's rheological behavior between different studies, most likely due to the sensitivity of the system to external parameters, such as pH and ionic strength.[11,12] This has not been made easier since lysozyme introduces a viscoelastic contribution at the air-water interface not representative of the bulk sample,[13] which is commonly present in rheometer-based measurements due to instrumental details and can lead to measurement artifacts.[14]

2.1.2 Crystallins

Crystallins is a collective term for different protein families with the prerequisite that they are all present in the eye lens, although they may be situated in other parts of the body as well.[16] The name crystallin allegedly originates from Berzelius[17] and describes the crystal clear appearance of the eye lens and encompasses a multitude of protein families with designations such as α-, β- and γ-crystallins (also being the order of extraction in a chromatography experiment). There exist several more crystallin families but these three are ubiquitous in all vertebrates although at different levels.[18] The body manufactures cells in the eye-lens with extremely high protein concentrations to achieve sufficiently strong refractive properties to focus light onto the retina.[19] During development these cells produce sufficiently high protein concentrations and subsequently expel the organelles from the cells to reduce undesirable scattering and enhance lens transparency.[20,21] The eye-lens continually grows throughout life with new layers of lens fiber cells being added to the outmost part resulting in a core (nucleus) consisting of embryonic cells.[22] This also has the side effect that the cells are no longer able to produce new proteins and thus rejuvenate the crystallin content. This leaves the lens susceptible to degenerative related diseases such as cataract.[23,24] Crystallins are inherently highly stable proteins but are nevertheless vulnerable to undesirable conformational changes.[25] As a way to combat this issue a large part of the protein content is that of α-crystallin which is a chaperone protein and can act as an inhibitor to protein denaturation.[26] Ultimately, it is necessary to investigate crystallin behavior and interactions at the concentrations they readily achieve in the eye lens to be able to understand their role in diseases. This is severely limited by the low availability and time consuming preparation procedure which hampers the achievable volumes for rheological investigations.

Alpha, α

The highly polydisperse α-crystallin (300 - 1200+ kDa, with an average of 800 kDa) consists of a mixture of the two subunits α_A and α_B.[26] The subunit α_B is found throughout the body acting as a chaperone protein while α_A appears to be almost exclusive to the eye-lens.[24] The amount of α-crystallin in the eye-lens can be as high as 50% of the total protein mass, where it acts, not only as a chaperone but also, as a structural protein.[26] The development of a protein degenerative disease such as age-related cataract is commonly attributed to an overall diminishing chaperone activity with time as the amount of α-crystallin, not already activated as chaperones, decreases.[24] It has been shown that α-crystallins behave as hard spheres at physiological buffer conditions.[27]

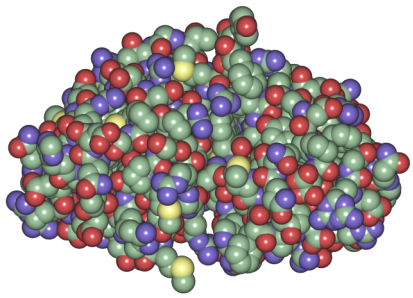

Figure 2.2: Atomic representation of the eye lens protein γ_B-crystallin. [31]

Beta, β

The smaller but still polydisperse β-crystallin is oligomeric and heterogeneous by nature and commonly divided in two groups called β_L and β_H separated by their molecular weight with β_H (160 - 200 kDa) [28] being used in this work. The β-crystallin subunits are closely related to γ-crystallin but their function in the eye-lens does not appear to be fully understood. [16] It is possible that its main function is that of a filler to maintain osmotic pressure in the lens while allowing for transparency and high refractive index. [29] There is work in literature claiming that β-crystallin display some form of repulsive interaction in solution, albeit this has not been thoroughly investigated yet. [29,30]

Gamma, γ

Although similar to the subunits of β-crystallin, the family of γ-crystallin consists of monomeric globular proteins but are not known to form larger species due to the lack of exposed terminal extensions. [23] Despite or due to their small size of approximately 20 kDa[32] they appear to have a vital effect on the refractive properties of the eye-lens. They are generally more prevalent in the lens nucleus resulting in a higher refractive index at the center than for the cortical. [18] This difference vanishes with age[33] and is proposed to explain the lens paradox[34], where a larger lens does not lead to enhanced vision. The high refractive index increment of γ-crystallin is also why it is extremely prevalent in the fish eye, with possible concentrations above 1000 g/ml, since the surrounding water requires a more elevated refractive index as compared to air-living creatures which have around 300 mg/ml. [35,36] It is thought that mutations in γ-crystallin and the accompanying interaction changes are the main causes of cataract in the eye lens[37,38] and its interaction behavior is thus of high scientific interest. The focus of the work on γ-crystallin presented in this thesis has been on the subtype γ_B-crystallin, also called γ_{II} and is shown in figure 2.2, which has been found to display short-range attractive interactions. [29,39–42]

2.1.3 Antibody

Antibodies[43] are part of the defense mechanism for biological systems to protect themselves against pathogens, such as bacteria and viruses. Due to their high moldability monoclonal antibodies, mAB, are highly desirable as biotic agents to target problematic entities, such as cancer cells, and induce an immune response in the body to destroy those cells.[44] A desirable goal is to produce these medical products in a way where they can be administered intraveneously thus being syringeable.[45] This requires high protein concentration to minimize the injected volume, leading to viscosity concerns that are difficult to quantify early in the research stage.[46]

2.2 Protein Preparation

2.2.1 Lysozyme

Lysozyme is commercially available and obtained as a lyophilized (freeze-dried) powder which was stored in the freezer as received. The buffer used consists of Hepes (4-(2-hydroxyethyl)-1-piperazineethanesulfonic acid) which is a zwitterionic agent and one of Good's buffers.[47] It is dissolved at a concentration of 20 mM in MQ-H_2O (Milli-Q, 0.22 µm) and a small amount of 1 M NaOH is added to adjust the pH to 7.80. Typically 1-1.5 g of lysozyme is dissolved in the buffer at a final concentration of 40 mg/ml. A magnetic stirrer is utilized as the powder does not readily dissolve without agitation. There is a surprising amount of salt present in the lysozyme powder and it is crucial to remove this to reach the desired condition of low ionic strength. The lysozyme solution is filtered using Acrodisc syringe filter (0.8/0.2 µm) directly into an Amicon Ultra centrifugal device with a 3 kDa filter. This device is initially used to remove the undesired salt by centrifugating the solution and rediluting the concentrated protein phase with filtered Hepes buffer. The conductivity of the discarded supernatant is monitored until it reaches the same level as the clean buffer, after which the protein solution is ready for use.

2.2.2 Crystallins

All crystallins are ultimately extracted from calf eyes which are obtained fresh from a slaughterhouse in Switzerland. The individual lenses are surgically removed and thoroughly washed in MQ-H_2O before being stored on ice. The low storage temperature induces cold cataract in the γ_B rich nucleus which turns opaque and easily distinguishable. The nuclear part is separated from the cortical (outer part of the lens) using the

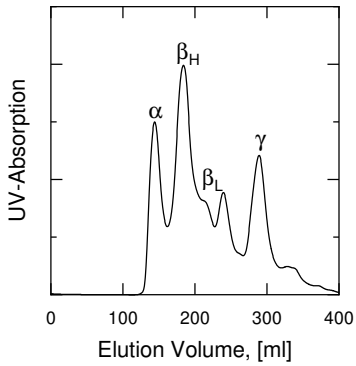

Figure 2.3: A typical SEC-chromatogram of the cortical extract allowing for extraction of α and β_H.

same principle as that of a punch-card system. The cortical fraction is stored in a 52.4 mM phosphate buffer, pH 7.1 (18.4 mM NaH_2PO_4, 34 mM Na_2HPO_4, 50 mM NaCl, 1 mM DTT (DL-Dithiothreitol), 1 mM EDTA (Disodium ethylenediaminetetraacetate dihydrate), and 0.02 wt% NaN_3). The additives are used to allow for long-term storage where DTT prevents proteins from forming sulfur bridges while EDTA prevents enzymatic activity by chelating divalent cations and NaN_3 is used to prevent bacterial growth. The nuclear fraction is stored in sodium acetate buffer with pH 4.5 and an additional 0.02 wt% NaN_3. Both of the collections are homogenized using a grinder which breaks the cellular walls and releases the protein content within. The resulting extracts are centrifuged to separate the protein solution from the undesired cellular components.

α and β_H

The cortical extract is filtered and passed through a size exclusion chromatography, SEC, column (HiLoad XK 26/60 Superdex 200 prep grade, GE Healthcare) with the chromatogram shown in figure 2.3. The fractions corresponding to α and β_H are collected and stored in the fridge.

γ_B

The filtered nuclear extract is passed through the same type of SEC column as the cortical with the fractions containing the mixture of different γ-crystallins, shown in figure 2.4a being collected. This mixture is then passed through a SP Sepharose fast

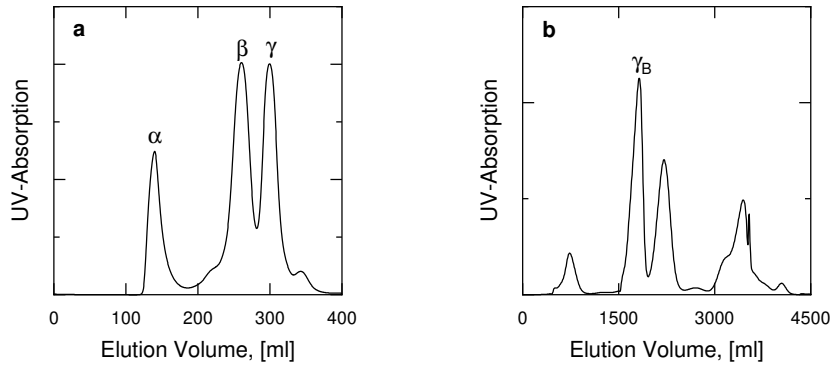

Figure 2.4: Typical chromatograms for the purification of γ_B **a**: SEC-chromatography of nuclear extract yielding a mixture of γ-crystallins. **b**: Subsequent IEX-chromatography allows for the extraction of γ_B.

flow ion exchange column, IEX, where the individual γ-crystallins are separated using a salt gradient, figure 2.4b, and the fractions corresponding to γ_B are collected. The protein is stored in the fridge but with the buffer exchanged to that used for α and β_H.

2.2.3 Antibody

The protein was received from Novo Nordisk at a concentration of 100 mg/ml in a 10 mM Histidine pH 6.5 buffer with an added 10 mM NaCl. The buffer was replaced with 20 mM Histidine pH 6.5 buffer, containing either an additional 10 mM or 50 mM NaCl, using illustra NAP-25 columns.

2.3 Concentration

The proteins were concentrated using Amicon Ultra centrifugal filters with cut-off at 10 kDa or 3 kDa and volumes 15, 3 or 0.5 ml as appropriate. The final concentrations were determined from UV-absorption at 280 nm. At least three aliquots were extracted from a sample, these acted as a quality check of the concentration determination, and diluted to get within range of the absorbance determination. The dilutions were monitored gravimetrically with the effect of protein content on the sample density accounted for

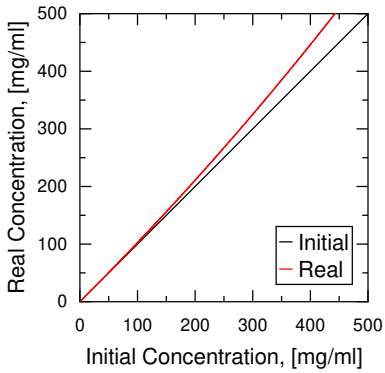

Figure 2.5: The change in protein concentration when accounting for the contribution from the protein to the total density of the sample.

using equation 2.1.

$$\frac{1}{c_{after}} = \frac{1}{c_{before}} + \left(\frac{1}{\rho_{protein}} - \frac{1}{\rho_{buffer}} \right) \tag{2.1}$$

Here, c_{before} and c_{after} are the concentrations before and after accounting for the density while $\rho_{protein} = 1.35$ g/cm^3 and $\rho_{buffer} = 1$ g/cm^3. The effect of this deviation due to the density contribution from the protein is shown in figure 2.5. Concentrations were finally converted to volume fractions (Φ) using the voluminosity of the protein when applicable.

There is only one item which is worth learning,
and that is the simple definition of viscosity
which we will come to in a moment.
The rest is only for your entertainment.
— Richard Feynman

CHAPTER 3

VISCOSITY

Contents

Viscosity can be seen as a measure of a material's willingness to flow, with higher viscosity meaning it is more reluctant to do so. Pouring a pitcher of water (low viscosity) on the kitchen table will lead to a wet floor while a placed dough (high viscosity), with the same amount of water but with added flour, will only spread modestly on the table. At the extremes of the viscosity range one finds materials such as super-cooled ^{4}He and pitch. When ^{4}He is sufficiently cold,[48,49] at temperatures below 2 K[50] it begins to show superfluid behavior, e.g. displaying zero viscosity. Such a fluid will flow completely unhindered and if one would stir it, it would continue to flow indefinitely.[51] On the other end, pitch appears to be completely solid when observed casually but has been shown to flow in the illustrious pitch-drop experiments.[52] The most famous one, initiated in 1927, contains a funnel with pitch placed over a beaker into which drops are collected, in April 2014 the ninth drop was recorded.[53]

3.1 Rheology

There are several good resources for an introduction to the field of rheology, either online[54] or in a multitude of text books.[55–57] One can broadly say that a material is described according to one of three categories (excluding special cases like Bingham plastics). The first, denoted Newtonian fluid, displays a pure viscous response and thus flows when exposed to external forces. It responds linearly to the applied stress, i.e. the viscosity is constant with respect to the induced stress, with water at ambient conditions being a common example. The second, called Hookean solid, displays a purely elastic behavior to applied forces, i.e. it stores the energy and releases it again once the force resides. An imperfect analogy would be that of a rubber band, once the pulling of such a band stops it will revert back to its original shape, assuming no material change has occurred during the applied stress. The third category displays viscoelasticity, i.e. something in between the previous two system types, which in practice encompasses basically everything of general interest. These materials can be called non-Newtonian fluids since they display non-Newtonian viscosity, i.e. the viscosity changes with applied stress and can either appear viscous or elastic depending on the force applied. If such a material is shear-thinning it will behave more fluid-like when the applied force is increased, e.g. ketchup. If it instead shows a more solid-like behaviour it is denoted shear-thickening with oobleck being a common example.

The viscosity of a fluid is determined by how easily the components of the fluid can pass each other, basically an internal friction, which in turn depends on interactions between them. For this reason, there will be a velocity gradient during flow where the motion will be hindered close to any external surface and gradually increase with distance from it. Two common ways to directly measure the viscosity of liquids is to use an Ostwald viscometer or a falling sphere viscometer. Both of these utilize gravity as the external force and record the time it takes for either the liquid itself or an immersed sphere to move a certain distance. These are limited in their investigative range by the corresponding choice of tube width and sphere dimensions. For samples displaying non-Newtonian behavior it is often preferable to utilize rheometers where the applied force can be varied to investigate the material's stress behavior. As these instruments measures the shear response of the sample one obtains the viscosity as a function of the shear rate which can then be extrapolated to infinitely low shear thus yielding the zero-shear viscosity. This is an important parameter for determining properties such as polymer molecular weight and long-term stability of suspensions.

3.2 "Hard Sphere" Systems

A system such as a protein solution can in its simplest state be described as a liquid containing particles at some concentration. Generalizing such a solution to isotropic and monodisperse particles with no ranged interactions results in the hard sphere system. There are a multitude of different models that aim to describe the viscosity-concentration behavior of hard spheres, from dilute conditions to close packing.[58,59] The phase diagram of such a system will only depend on the particle volume fraction, Φ,[60,61] as a change in for example temperature will not have a significant effect on a particle's ability to move. At sufficiently high concentrations, the diffusivity of a particle will become restricted by the close proximity of other particles, which eventually leads to the formation of nearest-neighbor cages[61–64] that physically hinders crystallization by restricting particle mobility.[60,65–67] This restriction of particle mobility is coupled with a viscosity increase of multiple magnitudes due to the systems increased inability to rearrange when exposed to external forces.[68–70] A hard sphere system in this concentrated regime is called a repulsive glass,[61,62,64,71–73] while its exact location is not without dispute[74–76] it is often taken as occurring at $\Phi_g = 0.58$ denoted the glass transition of the system.[64,67,70,77,78]

The change in viscosity with increasing concentration at very dilute conditions, thus neglecting interactions between particles, was early determined to follow a simple linear relationship called the Einstein equation[79,80] (Equation 3.1a) where η_r is the viscosity normalized with that of the solvent and $[\eta]$ is the intrinsic viscosity which takes the value of 2.5 for spherical particles. Efforts were later made to expand this relation into semi-dilute concentrations by adding higher order terms where the value of the second order coefficient depends on which forces are taken into account for the different models.[81] As these attempts were aiming for the semi-dilute region, none were able to capture the apparent divergence of viscosity a system displays when nearing the volume fraction corresponding to the arrest transition of the system, Φ_{max}.

One of, if not, the earliest investigator of this highly concentrated regime was Bernal who was interested in the structure of systems with concentrations between those of a gas and a crystal.[82,83] He used a macroscopic system of small metal balls packed in various containers that he froze in place using a fixating medium and proceeded to meticulously record the position of each individual ball.[84,85] This led to the determination of the random close-packed, rcp, limit of hard spheres, i.e. the highest concentration achievable without crystallization, at $\Phi_{rcp} = 0.64$.[84]

$$\eta_r = 1 + [\eta] \cdot \Phi \qquad \text{(Einstein)} \qquad (3.1a)$$

$$\eta_r = \exp\left(\frac{[\eta]\Phi}{1 - \Phi/\Phi_{max}}\right) \qquad \text{(Mooney)} \qquad (3.1b)$$

$$\eta_r = \left(1 - \frac{\Phi}{\Phi_{max}}\right)^{-[\eta]\Phi_{max}} \qquad \text{(Krieger-Dougherty)} \qquad (3.1c)$$

$$\eta_r = \left(1 - \frac{\Phi}{\Phi_{max}}\right)^{-2} \qquad \text{(Quemada)} \qquad (3.1d)$$

There appears to be especially three expressions, out of the many different models, that are immensely popular to describe the viscosity behavior over the entire range from dilute to highly concentrated. These were first described by Mooney[86] (Equation 3.1b), Krieger-Dougherty[87] (Equation 3.1c) and Quemada[88] (Equation 3.1d). Models that aim to describe the behavior even at high concentrations attempt to somehow account for nearness of particles such as crowding for Mooney and changes in flow properties for Krieger-Dougherty and Quemada. These three expressions all display an expected divergence at Φ_{max}, while equations 3.1b and 3.1c also reduces to equation 3.1a when $\Phi \to 0$. The different behaviour of these relations are visualized in figure 3.1 using the parameters $[\eta] = 2.5$ and $\Phi_{max} = 0.64$.

3.3 Non-"Hard Sphere" Systems

In reality, proteins can display widely different interaction potentials compared to the simple case of hard spheres. Proteins may for example carry a net charge caused by (de)protonation of certain amino acids distributed on the protein surface. Such a repulsive interaction, if between same-charge species, will shift the arrest transition to lower concentrations.[89,90] This is due to the extension of the electrostatics from the particle surface which yields an effective volume fraction, Φ_{eff}, (Equation 3.2) larger than Φ, by redefining the theoretical Φ_{max} with that which was measured.

$$\Phi_{eff} = \Phi \cdot \left(\frac{\Phi_{max}^{theory}}{\Phi_{max}^{measured}}\right) \qquad (3.2)$$

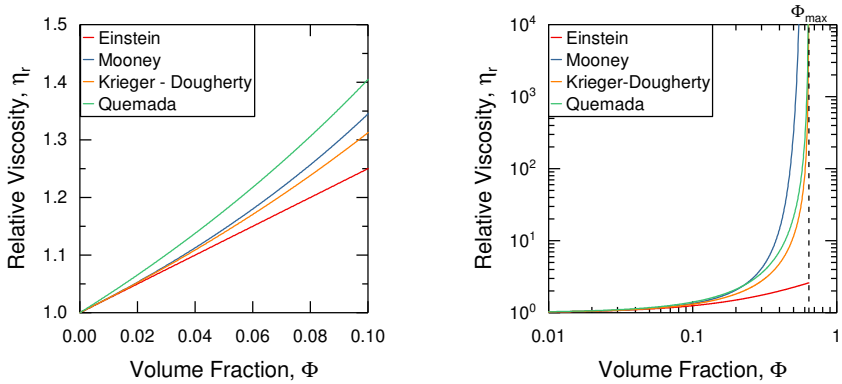

Figure 3.1: The different viscosity relations described in equations 3.1a-d with $[\eta] = 2.5$ and $\Phi_{max} = 0.64$. **a**: Low concentrations showing the overlap between equations 3.1a-c when $\Phi \to 0$, linear axis **b**: High concentrations showing the divergence when approaching Φ_{max}, logarithmic axis

The value of $\Phi_{max}^{measured}$ can be estimated from a plot of ${\eta_r}^{-0.5}$ vs Φ where a linear fit extrapolated to ${\eta_r}^{-0.5} = 0$, assuming the Quemada relation (equation 3.1d) holds.

A second difference is caused by the existence of hydrophilic/hydrophobic regions on the protein surface that result in short-range attractive interactions consequently leading to proteins sticking together at close contact. Systems displaying attractive interactions have been shown to display a power-law dependence of the viscosity (Equation 3.3), where the exponent ν depends on the attractive model used.[91–93]

$$\eta_r \propto |\Phi - \Phi_{max}|^{-\nu} \tag{3.3}$$

The existence of an attractive potential obfuscates the behavior at the liquid-solid transition and several experimental and theoretical studies have revealed the existence of a complex arrest line, which depends on the strength of attraction.[94–99] The presence of weak attractions leads to breakage of the nearest-neighbor cages, that governed the arrest of a hard sphere system, resulting in a liquid phase at concentrations where an arrested hard sphere system would normally be found. Increasing the attraction further, while keeping the concentration constant, leads to a reentrant arrest transition since the stronger attractions induce interparticle association,[63,92,97,98,100] a phase commonly called an attractive glass[61,62,64,70,72,73] which is suggested to differ from a gel by occurring at high volume fractions without the formation of a macroscopic network.[101–103]

Although both of these types of interactions can be achieved for large colloids using either charged surface groups or by the addition of small depletants (See Section 5.2

and Paper I for more information on depletion interaction), proteins offer a cleaner investigation of macroscopic phase behaviours, especially for attractive systems, as well as the opportunity to directly probe concentrated biological systems. For example, the phase behaviour of a system interacting via a combination of short-range attractive and long-range repulsive forces, SALR, (not uncommon among proteins) has a significantly more intricate phase behavior than that of hard spheres. For example, it has been shown that SALR results in the formation of equilibrium clusters[8] which was not expected and subsequently heavily debated.[104,105] Investigating the formation and behavior of proteins that display a cluster phase is highly desirable in order to understand protein crystallization as well as for medicines based on monoclonal antibodies where clusters can have a significant impact on manufacturing and administration procedures.[106,107]

Look again at that dot. That's here.
That's home. That's us.
— Carl Sagan

CHAPTER 4

LIGHT SCATTERING

Contents

Light scattering as a concept describes an interaction where the incoming light commonly leaves at a direction different than from where it entered. This can easily be observed for example within a ray of sunlight passing through a dusty room. Scattering of an electric field occur due to local changes in polarizability of the irradiated sample originating from the difference in refractive index between the scatterer and surrounding medium. This is in contrast to absorption where the incoming light is instead incorporated into the absorber. One generally speaks of two types of scattering, elastic and inelastic, depending on whether the kinetic energy is conserved or partly transformed. When one talks about light scattering of particulates in solution, such as proteins or microspheres, it refers to elastic scattering. The light source of choice for scattering experiments is a laser since it fulfills the requirements of monochromatism and minimal divergence over the length of a sample. Depending on the relative size difference between the scatterer and the wavelength of the light one generally distinguishes between two different scattering regimes. The first, Rayleigh scattering occurs when the wavelength of light is much larger than the scatterer and is famously responsible for making the sky blue as shorter wavelengths are scattered more predominately. The other regime is Mie scattering and occurs when the scatterer size is on the same order as the wavelength which, in turn, is responsible for the whiteness of clouds since there is no longer any wavelength dependency on the scattering of visible light.

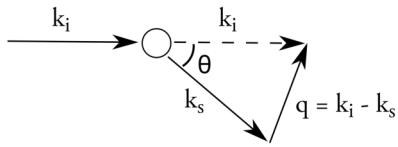

Figure 4.1: Geometrical representation of the scattering vector described in equation 4.1.

A detailed overview of scattering phenomena, including light scattering, can be found in "Neutrons, X-Rays and Light"[108] and similar text books. More easily available descriptions can be found in various publications.[109–111]

4.1 Static Light Scattering

A scattering event from a point scatterer can be described with a scattering vector, $\vec{q}$, which is shown in equation 4.1 and details the directional difference of the scattered light.

$$\vec{q} = \vec{k}_i - \vec{k}_s \tag{4.1}$$

The subscripts i and s of the wave vector, $\vec{k}$, denote the incoming and scattered light respectively as shown in figure 4.1.

It is geometrically possible to calculate the magnitude of $q = |\vec{q}|$ by knowing the scattering angle, θ, using equation 4.2.

$$q = 2|\vec{k}|\sin\left(\frac{\theta}{2}\right) \tag{4.2}$$

Here $|\vec{k}| = \frac{2\pi n}{\lambda}$, where n is the medium refractive index and λ the wavelength.

As soon as the theoretical point scatterer is replaced with a physical object that has some extension in space the angular scattering profile will contain information that describes the shape of the scatterer. This contribution is called the form factor and, in the case of material homogeneity of the scatterer, can be written as equation 4.3

$$P(\vec{q}) = \left[\frac{\int e^{-i\vec{q}\cdot\vec{r}}\,dV}{V}\right]^2 \tag{4.3}$$

where $\vec{r}$ denotes the relative location of two scattering elements in the scatterer with the integral being over the entire particle volume, V. This property can be measured with static light scattering, SLS, if the sample is dilute enough such that there is no structural component. In the case of spherical scatterers there exists an analytical solution to this expression which is shown in equation 4.4,

$$P(q) = \left[\frac{3}{(qR)^3} \left(\sin(qR) - qR \cdot \cos(qR) \right) \right]^2 \tag{4.4}$$

with R being the radius.

4.2 Dynamic Light Scattering

In addition to the static component there also exists a temporal or dynamic component in the scattering profile which is averaged away in SLS-measurements. This dynamic component can be investigated using dynamic light scattering, DLS, and arises from interference fluctuations caused by the thermal, Brownian, motion of the suspended scatterers and is directly dependent on the diffusion of scatterers within the medium. These fluctuations will induce a system memory decay that can be described by the field autocorrelation function, $g^{(1)}$, shown in equation 4.5 for a certain q

$$g^{(1)}(\tau) = \frac{\langle \mathbf{E}(t)\mathbf{E}^*(t+\tau) \rangle}{\langle \mathbf{E}(t)\mathbf{E}^*(t) \rangle} \tag{4.5}$$

where t and τ are time components and **E** the scattered electric field. It is not possible to directly measure the scattered electric field, however by monitoring the scattered intensity it is possible to construct the intensity autocorrelation function, $g^{(2)}$, displayed in equation 4.6

$$g^{(2)}(\tau) = \frac{\langle I(t)I(t+\tau) \rangle}{\langle I(t) \rangle^2} \tag{4.6}$$

where the intensity $I(t) \propto |E(t)|^2$ which eventually yields equation 4.7.

$$g^{(2)}(\tau) - 1 = B \left[g^{(1)}(\tau) \right]^2 \tag{4.7}$$

This equation is also called the Siegert relation and describes the relation between the two autocorrelation functions with B being the recorded intercept of the intensity auto-

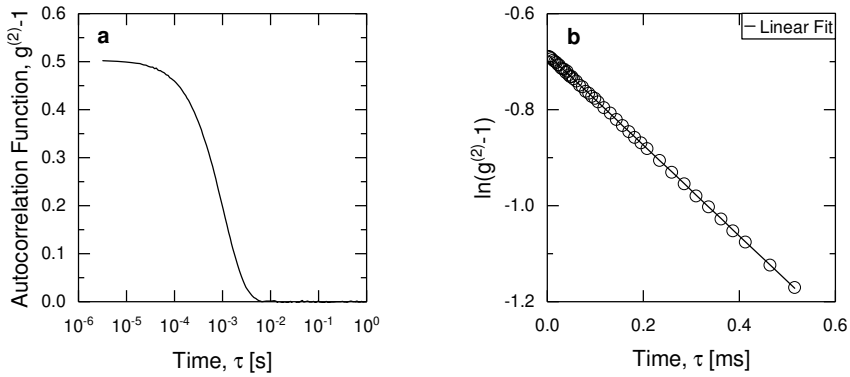

Figure 4.2: **a**: Intensity autocorrelation for a dispersion of polystyrene particles. **b**: A linear fit to the logarithm of the initial slope of the decay in **a** which is used to determine μ_1.

correlation function. Figure 4.2a shown an example of an autocorrelation function for polystyrene particles with a diameter of 0.3 µm.

This can be related to physical characteristics of the scatterers through equation 4.8

$$g^{(1)}(\tau) = \int_0^\infty G(\Gamma) e^{-\Gamma\tau} \, d\Gamma \tag{4.8}$$

with $G(\Gamma)$ being the population distribution of scatterers with decay constant Γ.

The correlation function is most easily analyzed using equation 4.9 which describes the cumulant expansion[112,113] of $g^{(1)}$

$$\ln(g^{(2)}(\tau) - 1) = \ln\left(B\left[g^{(1)}(\tau)\right]^2\right) = \ln(B) + 2\left(-\mu_1\tau + \frac{\mu_2}{2}\tau^2 - \frac{\mu_3}{6}\tau^3 + \ldots\right) \tag{4.9}$$

where μ_x are the cumulant coefficients. Figure 4.2b shows the natural logarithm of the initial slope of Figure 4.2a together with a linear fit used to extract μ_1.

The first order cumulant coefficient depends on the diffusion coefficient, D, of the scatterer as described by equation 4.10.

$$\mu_1 = q^2 D \tag{4.10}$$

The diffusion coefficient is related to the particle size and sample conditions according to the Stokes-Einstein relation shown in equation 4.11

$$D = \frac{k_B T}{6\pi\eta R_H} \tag{4.11}$$

where $k_B T$ is a measure of the thermal energy, η is the medium viscosity and R_H the hydrodynamic radius of the scatterer.

The higher order cumulant coefficients are related to other properties of the population distribution, with μ_2 being related to its width while μ_3 and μ_4 are related to the skewness and kurtodis respectively. The polydispersity index, PDI, of the scattering population can be determined from the second order coefficient using equation 4.12.

$$PDI = \frac{\mu_2}{\mu_1^2} \tag{4.12}$$

4.3 Multiple Scattering

The theory of light scattering presented here assumes dilute scattering conditions where the scattered light recorded by the detector is singly scattered. This refers to the scattering region where the mean free path is much larger than unity, i.e. $l/L \gg 1$ where l is the average distance a photon covers before being scattered and L is the total sample length.[114] Once this definition no longer holds, i.e. when the concentration of scatterers is elevated, the sample will display turbidity, or cloudiness. This originates from the, no longer insignificant, chance of the singly scattered light encountering another scatterer before reaching the detector. Scattering is therefor no longer localized solely in the volume traversed by the laser but may reach the detector from different undesirable locations within the sample. This affects SLS measurements by smearing the scattering profile as the form factor minima will now also contain an extra component due to multiply scattered light. For the same reason, DLS measurements may suffer from a reduction of the autocorrelation intercept as the intensity trace will contain uncorrelated signal.

The definition of the mean free path also contains the two most obvious ways of reducing multiple scattering, namely increasing l by diluting the system or decreasing L, i.e. utilizing a thinner sample container. Sometimes neither of these are valid options and a choice is then to remodel the entire experimental setup. One option is the use of a dual laser setup with two different wavelengths that are recorded by individual detectors sensitive to either of the wavelengths.[115] It is then possible to perform

two scattering experiments simultaneously in the same scattering volume by carefully selecting the angular arrangement of the lasers and detectors. Any multiply scattered light will originate from different parts of the sample for each of the measurements and can thus be removed by cross-correlating the two signals.[63,114]

Another method for suppressing the influence of multiple scattering is the use of a 3D-setup.[114,116] Here, instead of utilizing different wavelengths one exploits the third vertical dimension. The incoming laser light is split in two parts that enter slightly above and below the normal scattering plane, likewise the detectors will also be offset from the plane. Similar to the two-color setup this allows for the simultaneous measurement of two scattering experiments by cross-correlating the two signals, albeit with more limitation since the detectors are unable to differentiate between the two experiments. Although this allows for measurements of turbid samples there is an inherent 4x reduction of the correlation intercept due to cross-pollution of the two signals. As a way to combat this issue, the instrument can utilize a modulation arrangement where the incoming light, after being split in two beams, is alternately blocked thus creating a temporal difference between the two experiments which allow for cross correlation without cross-pollution.[117] However, this has the side effect of restricting the accessible short time range as motion faster than the modulation time will not be resolvable.

This type of setup was used for the work in this thesis and utilized a 3D-LS Spectrometer (LS Instruments AG, Switzerland) equipped with a goniometer for the detector stage, allowing for easily changing the scattering angle, as well as a second goniometer for sample rotation. The setup was initially equipped with a He-Ne laser with $\lambda = 632.8$ nm but later remodelled with a Cobolt Flamenco diode laser with $\lambda = 660$ nm. The sample temperature was controlled using a water-cooled vat containing decalin.

I can dive and swim in these coins like they were water.
— Scrooge McDuck

CHAPTER 5
MICRORHEOLOGY

Contents

Microrheology as a concept relies on observing the motion of microscopic tracer particles in a particular sample of interest and can utilize vastly different techniques that are encompassed by their use of low sample volumes.[118–125] This can be achieved indirectly using different forms of light scattering setups or directly by recording the motion using video microscopy. The second method can be augmented with special instruments, such as optical trapping, to actively subject the tracer particles to external forces, i.e. active microrheology. This allows for probing the nonlinear response of a sample which is not achievable when measurements rely solely on the inherent thermal motion of the tracer particles, i.e. passive microrheology.

5.1 Background

Microrheology was early successful in investigating polymer and emulsion based systems and much of the theoretical framework was demonstrated using these systems.[126–134] There has been considerable effort over the last couple of decades to move to biologically interesting systems, such as proteins.[135–144] Here, the advantage of microscopic sample volumes would have a pronounced benefit over conventional rheology methods due to the, often, limited sample availability. However, this opens up several areas of concern not immediately present for more chemically inert systems such as polymers. First and foremost, there ought to be no (or at least non-influential) interactions between tracer particles and the protein to properly probe bulk rheological properties. Another concern is the solvent conditions which for proteins tend to be some type of buffering system where the presence of salt may induce particle aggregation in the case of electrostatically stabilized particles. Section 5.2 and Paper I further address the issue with particle stability. The majority of work on tracer particles for biological systems that show the most promising results use sterically stabilized particles[135,136,142–144] to solve both of these issues at once but other methods have been proposed and tested. One such method relies on predisposing the tracer particles to a secondary protein solution (commonly bovine serum albumin, BSA) to saturate any possible sites of interaction before subjecting them to the protein sample of interest.[135,137,145,146] Here, for example, two studies using the BSA-method on systems consisting of F-actin networks found conflicting results, where BSA either failed[135] or succeeded[137] in preventing particle adherence to the protein network. Another option is simply using charge stabilized particles but this method is understandably often associated with poor results.[135–137,139,142,143]

An important application of microrheological techniques is the ability to non-invasively and continuously investigate evolving systems, such as aging soft colloids,[147] cross-linking of polymers,[148,149] aggregation of protein[150] and gelation of milk.[151] A more exotic application is investigating the viscoelasticity of the cytosol in cells as it will have profound implications on the transport of cellular components. Fluorescent molecular rotors have for example been used to investigate the increase in viscosity upon cell death.[152] Particle tracking microrheology has been utilized to probe the inner workings of living cells[153] as well as track the diffusion of pharmaceutical nanocarriers within cells.[154] The method has also been used to investigate gravitropism which governs the orientational growth of plants.[155]

The two scattering techniques commonly used for microrheology are DLS and diffusing wave spectroscopy, DWS, which differ on whether single or multiple scattering is dominating. DWS[128,156] has the advantage of probing much higher frequencies than what is accessible with DLS and even bulk rheology.[122,133] In doing so it also requires

much higher concentration of scatterers as it relies on the "random walk"-like nature of the scattered light, achievable once the number of multiple scattering events is sufficiently large.[157] Due to this requirement the technique is readily used for samples that, by themselves, scatter much such as emulsions,[158,159] colloidal dispersions[160,161] and micellar solutions[151,162]. In contrast, DLS (described further in section 4.2), requires single scattered light and is thus confined to, at least sufficiently, transparent samples. This therefor limits the type of systems that can be investigated, but with the benefit that the data generated is more easily handled.

Passive microrheology based on video recording[120,123,124,163,164] tends to exploit the specialized technique commonly described as confocal microscopy. An ordinary light microscope collects all the 3D spatial information in a sample as a 2D projection on the objective. Confocal microscopy[165–167] utilizes a special lens arrangement to discard all information outside a specific plane of interest. This is highly useful for recording 3D structures, such as colloidal crystals and gels, as they can be imaged one plane at a time. For microrheology the setup allows for the recording of a tracer particle's mean squared displacement in two dimensions, 2D-MSD, where particles are discarded once they move sufficiently far in the third dimension and out of the plane. The properties of the extracted MSD will show whether the sample behaves as a Newtonian fluid (viscous), a Hookean solid (elastic) or something in between (viscoelastic). A MSD displaying viscous behavior can for example be used to calculate the diffusion coefficient of the tracer particle.[120,124] The benefit of a direct method, such as microscopy, is that problems, such as particle aggregation,[142] will be directly apparent. The drawback is that it can be time consuming to analyze (and record) enough videos to get sufficient statistics for bulk characteristics.[120,124] There is also a limitation as to how fast particles will move in low-viscous systems which may lead to difficulties of tracking particles between frames as well as how long they remain in the imaging plane which may reduce the statistics.[124]

All of the aforementioned techniques utilize passive microrheology which inherently probes the linear response of a sample.[124,125] This allows for the determination of parameters such as the zero-shear viscosity, assuming a diffusive system, without the need for extrapolation from non-zero shear as necessary for shear-based techniques such as rheometers.

5.2 Particle Stability

Particles are prone to aggregation if they lack long range repulsive interactions such as electrostatics or if these interactions are screened due to the ionic strength of the medium. This is caused by different intermolecular forces commonly collated as van

der Waals forces[168,169] that are short ranged and will thus be mitigated if particles can be kept sufficiently far from each other, using for example steric repulsion. In 1937, Hamaker presented an estimate of the attractive force between two spheres of identical size, shown in equation 5.1,

$$E = -\frac{A}{12}\left[\frac{y}{x^2+xy+y} + \frac{y}{x^2+xy+x+y} + 2\ln\left(\frac{x^2+xy+x}{x^2+xy+x+y}\right)\right] \tag{5.1}$$

where A is the Hamaker constant, $x = \frac{d}{2\cdot R_1}$, $y = \frac{R_2}{R_1}$, d is the surface-surface distance between particles and R_x the corresponding radius. This is described in more detail in Paper 1.

One possible concern with microrheology applied to protein systems is that samples will contain a mixture of (at least) two species, proteins and particles, that differ in size. Such a combination is known to induce a short range attractive potential between the larger species called depletion interaction.[170–174] In the case of microrheology this could become a problem if two tracer particles get sufficiently close such that the particle-particle surface distance is less than the size of the protein. The difference in osmotic pressure caused by the different protein concentrations in the region between the particles and that of the bulk will drive solvent to the bulk and thus force particles together. Depletion interaction with respect to microrheology is further discussed in Paper 1 and the accompanying supporting information. This phenomenon is commonly exploited in colloidal systems with the addition of small polymers to mimic short range attractions present in for example different protein systems.[8,64,171] The strength of the depletion interaction can be estimated from the Asakura-Oosawa-Vrij model shown in Equation 5.2

$$\frac{E}{k_B T} = -\left(1+\frac{R_{particle}}{R_{depletant}}\right)\cdot\left(1-\frac{3}{4}\chi+\frac{1}{16}\chi^3\right)\cdot\Phi_{depletant} \tag{5.2}$$

where χ is displayed in equation 5.3.

$$\chi = \frac{d}{R_{particle}+R_{depletant}} \tag{5.3}$$

5.3 Particle Preparation

All the particles used were obtained from ThermoFischer Scientific and received as carboxylate modified polystyrene spheres at concentrations 2-4 wt%. The dispersions with fluorescent particles were discovered to contain a nonionic surfactant, Tween, which had been used by the manufacturer during the swelling procedure where fluorophores were incorporated into the polystyrene matrix. The presence of Tween appeared to have a detrimental effect on the preparation procedure and was therefor initially removed by means of dialysis using Slide-A-Lyzer mini dialysis device, 20 kDa, against MQ-H_2O.

These electrostatically stabilized particles were then treated to create sterically stabilized tracer particles to minimize interactions with the protein being investigated while also providing enhanced particle stabilization in buffers with non negligible ionic strength. A schematic of the full procedure is displayed in figure 5.1 and detailed in Paper II. The concept is based on amine-coupling using EDC (N-(3-dimethylaminopropyl)-N'-ethylcarbodiimide) commonly used for cross-linking chemistry.[175,176] Amine-terminated PEG (polyethylene glycol) are covalently linked with carboxylic groups on the particle surface forming amide bonds in a MES-buffer[177] (2-(N-morpholino)ethanesulfonic acid) at pH 6. The dispersion was continuously agitated during the incubation to avoid particle sedimentation which otherwise appeared to interfere with the treatment, most likely by restricting the physical access of the reagents due to the relatively firm packing of particles in a sediment. Once completed, centrifugation was used to wash away remaining reagents from the particles using MQ-H_2O, with the final dispersion being stored in the fridge with an additional 0.02 wt% NaN_3 for longevity.

Evaluation of the cross-linking initially relied on the change in ζ-potential but was eventually improved to also evaluate particle stability as described in Paper II. The ζ-potential[178] can be used as a measurement of the amount of charges in a system and should have a high net value for electrostatically stabilized colloidal dispersions to prevent aggregation. As such, the particles ought to have a high value of the ζ-potential before the cross-linking with PEG and afterwards a value close to 0. Measurements were carried out on a Malvern Zetasizer Nano which employs electrophoretic light scattering to measure the change in mobility with an applied electric field. The measuring cell consists of a U-shaped capillary, where the measurement is performed at the bend and the end points contain the electrodes. A reduction in ζ-potential infers that the cross-linking is successful, at least to some degree, but does not mean that particles are stable against aggregation. As a verification of this, pegylated particles were dispersed in a salt solution with high ionic strength to screen any potential remaining charges. The hydrodynamic radius of the particles in such a dispersion was then continuously

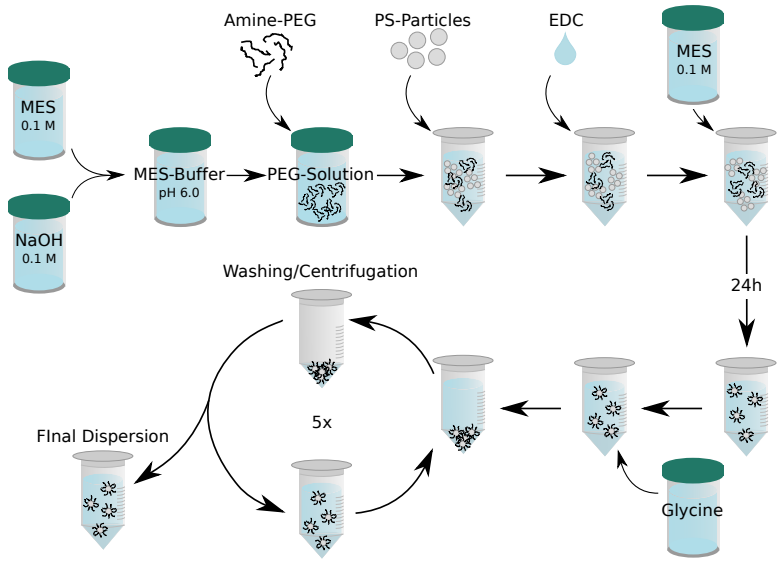

Figure 5.1: Experimental scheme of the procedure used for creating pegylated tracer particles detailed in Paper II.

measured using DLS, where a stability failure would show up as an apparent growth in particle size which is further detailed in section 6.1.2.

5.4 DLS-Microrheology

5.4.1 Theory

Reviewing equation 4.11 shows that the observed diffusion coefficient depends solely on the sample viscosity if the temperature and probe size are maintained. It is thus straightforward to extract the viscosity of an unknown sample as long as the diffusion coefficient of the corresponding tracer particle in a reference dispersion is known, i.e. as shown in equation 5.4 where η_r is the relative viscosity.

$$\eta_r = \frac{\eta_{sample}}{\eta_{reference}} = \frac{D_{reference}}{D_{sample}} \tag{5.4}$$

This method is valid as long as the Stokes-Einstein relation is applicable, i.e. the sample behaves as a Newtonian fluid and the tracer motion is purely diffusive. The diffusion coefficient is a measure of the MSD, $\langle \triangle r^2(\tau) \rangle$, of the diffusing particle according to

equation 5.5

$$\langle \triangle r^2(\tau) \rangle = 2i \cdot D \cdot \tau \tag{5.5}$$

where i is the dimensionality of the diffusion and is equal to 3 for DLS as long as the scattering is isotropic. Using the cumulant expansion, equation 4.9, of first order together with equation 4.10 shows that the field correlation function can be written as equation 5.6

$$g^{(1)}(\tau) = e^{-q^2 D \tau} \tag{5.6}$$

Equations 5.5 and 5.6 can then be combined to allow for the extraction of MSD from a DLS-experiment[122,179] as shown in equation 5.7

$$\frac{g^{(1)}(\tau)}{g^{(1)}(0)} = e^{\langle \triangle r^2(\tau) \rangle \cdot q^2/6} \tag{5.7}$$

5.4.2 Methodology

The methodology of DLS-microrheology is detailed in Paper II. All DLS-measurements were performed using 5 mm NMR tubes as sample holders to minimize the amount of protein needed. These were initially cleaned with 99.7% ethanol and MQ-H_2O, and then left to dry upside down to minimize the risk of contamination from dust. The sample was initially prepared in a 0.5 ml lo-bind eppendorf tube already containing the protein, usually a volume ~ 100 µl. Particles (< 10 µl) were added directly to the eppendorf tube which was immediately vortexed to homogenize the sample. Due to the low sample volume[134] this step was sometimes problematic when the protein concentration was high and it could be necessary with prolonged vortexing over several minutes. This also turned out to be a limiting factor for how high sample concentrations that were possible to reach. The new, slightly lowered, protein concentration was calculated from the change in weight upon addition of the particle dispersion. The sample was then transferred to a clean 5 mm NMR tube using an automatic pipette with lo-bind tips. In the case of very high protein concentrations pipette tips with wide orifices were used and it was sometimes necessary to spin the sample down using a mild, brief centrifugation.

Microrheology measurements were most often performed at a scattering angle of 90° for 3-30 min depending on the sample viscosity, i.e. protein concentration. A reference dispersion of tracer particles without protein was always measured as well and used to

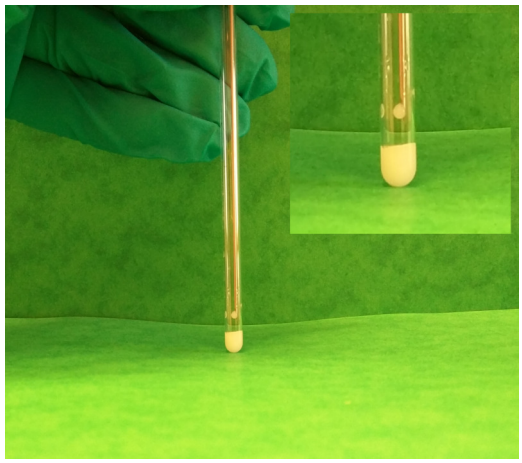

Figure 5.2: Example of how a dilution of the protein sample is performed directly in the light scattering tube using a syringe and a long needle to deposit particle dispersion above the meniscus.

extract the relative viscosity as explained in section 5.4.1. In an effort to reduce the amount of protein, an in-situ dilution method was conceived where a starting sample was diluted directly in the NMR tube several times, usually up to 4 or 5 for concentrated samples. This was achieved using a syringe and a long needle to place a small drop of the reference particle dispersion just above the sample meniscus without touching the sample with the needle (Figure 5.2). The volume added tended to be between 5-40 µl depending on how big of a concentration change was desired. The maximum total dilution was limited to about a factor 0.5 of the original sample concentration due to the thermostatted bath where a too large sample size would not be fully immersed anymore.

5.5 Multiple Particle Tracking

5.5.1 Theory

The computational models are detailed in the supporting information of Paper III and accompanying references.[123,142,180,181] The location and thus the motion of particles are extracted from a series of still frames finally yielding the mean squared displacement. The probability distribution (van Hove self-correlation) of particles having traveled a certain distance in a specific time was analyzed to find the time where the statistical properties were optimized. This time was then used to extract the diffusion coefficient of the tracer particles.

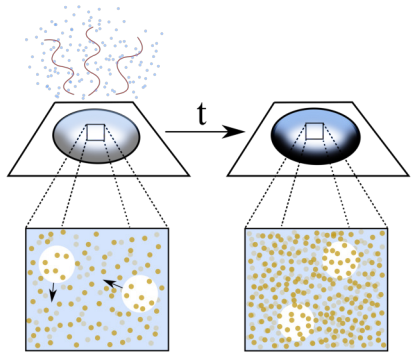

Figure 5.3: Simplified scheme of methodology where the protein (small spheres) concentration is increased by evaporating the solvent in a small sample volume leading to arrested tracer particles (large spheres)

5.5.2 Methodology

All multiple particle tracking, MPT, measurements were carried out on a confocal laser scanning microscope, CLSM Leica DMI6000. Samples with protein and fluorescent particles were initially prepared in the same way as for DLS-samples described in section 5.4.2. Circular sample wells were employed using sticker cells on microscope glass slides. A sample volume of 5 µl was deposited in the well and the cell sealed using a glass cover slip.

An unconventional method was designed in an effort to reach protein concentrations not directly accessible with the method described in section 5.4.2. This utilized the minute sample volumes applicable in MPT by allowing a controlled amount of time between sample deposition and sealing of the cell as visualized in Figure 5.3. The evaporation was tracked by performing the procedure on a sensitive balance and the new higher protein concentration determined from the reduced weight. This allowed for creating protein concentrations far into the arrested region with embedded particles.

The best way to treat obstacles is to use them as stepping-stones. Laugh at them, tread on them, and let them lead you to something better.

— Enid Blyton

CHAPTER 6

SUMMARY OF RESULTS

Contents

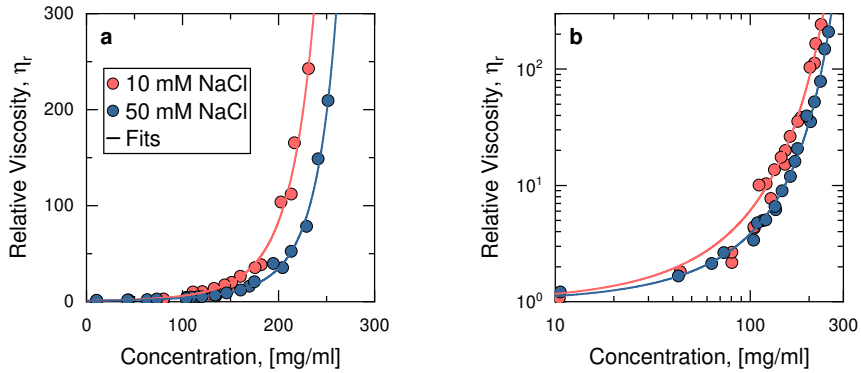

Figure 6.1: The effect of salt on the sample viscosity of mAB-solutions, demonstrating a shift to higher concentrations with increasing ionic strength. Fits are with the Mooney relation (equation 3.1b) except with concentrations instead of volume fractions. **a:** Linear axis **b:** Logarithmic axis

6.1 Tracer Particles

6.1.1 Initial Test with mAB

The choice of tracer particles for reliable microrheology investigations turned out to be more involved than initially expected. As detailed in section 5.1, there exists a vast repertoire of more or less successful variants in literature. It was rapidly realized that a system consisting of polystyrene particles, sterically stabilized with PEG had the highest chance of success. Initially a combination of 1.0 µm polystyrene spheres and 0.75 kDa PEG was tested, akin to that by Valentine et al.[135] This system was subsequently used to study a type of mAB and determine how salt affected the viscosity-concentration dependency and thus the location of the arrest transition.

It is desirable to obtain such information early in the pharmaceutical research phase as it relates to parameters such as syringeability, discussed in section 2.1.3. One would preferably see that the divergence of viscosity, occuring when near the arrest transition, appears at high protein concentrations as this allows for easier injections of small volumes during drug administration. A possible way to shift this divergence to higher concentrations while maintaining the protein composition is by means of additives, such as salt which screens long range electrostatic interactions between proteins. It is clear from figure 6.1a that the onset of the divergence occurs at a higher concentration with increasing salt concentration as expected. The accompanying fits are obtained using the Mooney relation, equation 3.1b, but only give a good agreement for the 50 mM data set, for which the maximum concentration comes out around 510 mg/ml.

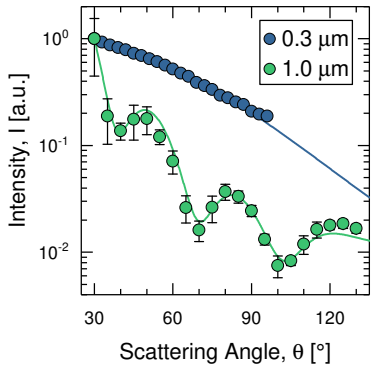

Figure 6.2: Experimental (circle) and theoretical (line) form factors displaying no minima for the smaller particles and several for the larger particles.

The data set for 10 mM NaCl gives an arrest concentration of 650 mg/ml but, as seen in figure 6.1b, the fit does not reproduce the data at lower concentration which also appears to be significantly more noisy and is thus inherently less reliable.

These initial tests with mAB were performed at both low particle concentrations and scattering angles (46-50°). Despite the low angle there was still a significant amount of protein signal in the autocorrelation functions. However, the large size discrepancy between the two scattering entities allowed for fitting only the long decay belonging to the particle signal. These experiments verified that the method was in principle working as it was possible to see a difference between the two salt concentrations. However, several issues became apparent, such as the influence of protein scattering, particle form factor affecting the choice of scattering angle as well as particle instability where aggregation appeared to be an increasing issue with time.

6.1.2 Revising the Tracer Particle System

The motivation for the alteration of the tracer particles is detailed in Paper 1. First of all, the existence of form factor minima was found to significantly complicate measurements as it became necessary to carefully choose the scattering angle to avoid these regions. The benefit of having a large size difference between tracer particle and protein is of course that scattering is strongly dependent on size, for example in the Rayleigh-region the scattered intensity depends on the size to the 6^{th} power. Reducing the particle size to 0.3 µm completely removed the concern of avoiding form factor minima, as seen in figure 6.2, while still maintaining a relatively large size difference between

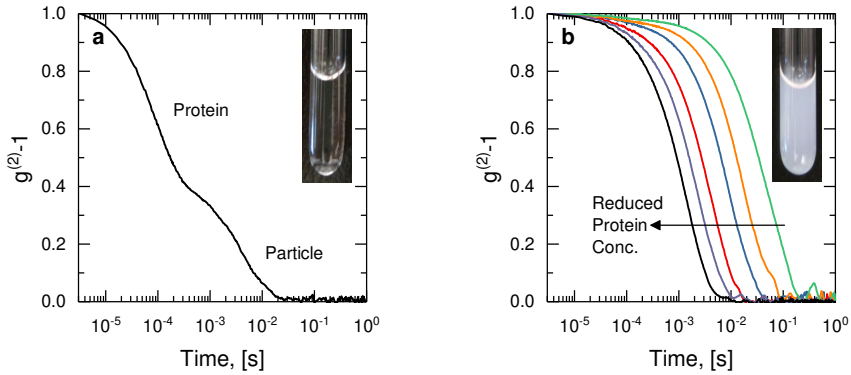

Figure 6.3: The effect of concentration on the DLS correlation function. **a:** Low particle concentration with a significant degree of protein scattering in the total scattering signal. Inset: Highly transparent sample. **b:** High particle concentration resulting in a dominating scattering signal. The shift of the decay constant reflects different protein concentrations. Inset: Sample displaying turbidity due to increased multiple scattering.

particle and protein. The experimental form factor of the smaller particles agreed well with that obtained from equation 4.4, while the larger 1.0 µm particles were best described using Mie theory[182] with a size of 0.92 µm.

Perhaps the main draw-back of shifting to a smaller particle size is the reduced difference in decay constants between the particle and protein. This can lead to situations where it will be difficult to properly extract information exclusively from the tracer particles without contributions from the protein. Figure 6.3a shows a sample where the particle concentration is so low that the protein contribution becomes significant. This was alleviated by increasing the particle concentration sufficiently such that it dominated the total scattering profile, as seen in figure 6.3b. This also shows the shift of the particle decay with reduced protein concentration due to the accompanying change in viscosity. The enhanced particle concentration resulted in a much more turbid sample, insets in figure 6.3, which directly lead to the need of employing the 3D cross-correlation technique to suppress the accompanying multiple scattering, further discussed in section 4.3. This increase in concentration also confirmed a suspicion that despite being pegylated the particles were not thoroughly sterically stabilized after all. An example of this is shown as red circles in figure 6.4a where a dispersion of 0.3 µm particles treated with 0.75 kDa PEG was monitored with DLS over time. The apparent size increase with time is a clear sign of particle aggregation meaning this PEG is not sufficient as a stabilizing agent.

If particles are allowed in close proximity they may aggregate due to intermolecular van der Waals forces as described in section 5.2. Figure 6.4b shows the range of these

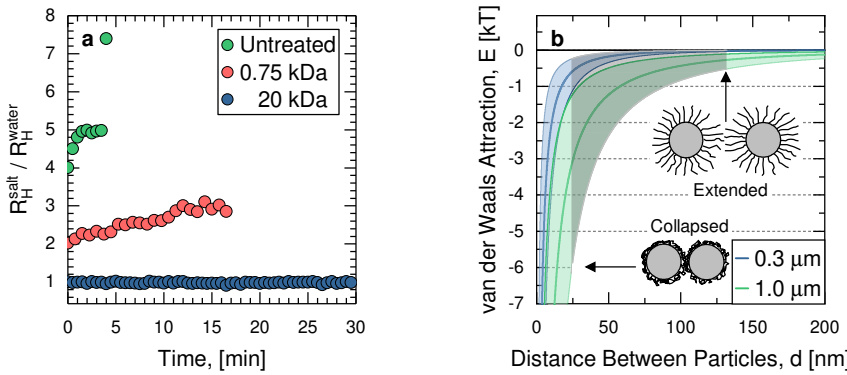

Figure 6.4: a: Continuous DLS measurements revealing aggregation as an apparent increase in size. Particles, 0.3 µm, dispersed in high ionic strength solution (green and blue) or low ionic strength buffer (red). **b:** Calculated van der Waals attraction for the two different particle sizes. The shaded region indicates the possible extension of the 20 kDa PEG depending on solvent quality.

attractive forces calculated using equation 5.1 for the two particle sizes thus providing further motivation to use a smaller particle size. The coloured areas indicate possible spread due to varying values of the Hamaker constant obtained from literature with the lines reflecting an average values, which is explained in more detail in Paper I. The obvious way to prevent this type of aggregation is to provide a repulsive force with sufficient range to counteract the attraction. It is clear that the 0.75 kDa PEG is not sufficiently large to achieve this requirement. The shaded region in figure 6.4b details the potential range of a much larger 20 kDa PEG shell depending on how extended the chains would be, which suggests that 20 kDa should be sufficient to sterically stabilize at least the 0.3 µm particles. This was also found to be the case as shown in figure 6.4a where particles treated with 20 kDa PEG (blue circles) and untreated particles (green circles) are dispersed in a high concentration of NaCl-solution to completely screen any electrostatic interactions. The treated particles show no signs of aggregation thus verifying that this larger PEG size is a more suitable option. It was also realized that literature describing the use of PEG to create anti-fouling surfaces noted the necessity of using high molecular weight PEG, preferably tens of kDa, to prevent protein adsorption which further validated this particle composition.[183–185]

Extending the procedure to fluorescent 0.2 µm polystyrene particles was initially unsuccessful. As it turned out, during the production step the manufacturer utilizes a swelling/deswelling procedure using organic solvents to incorporate the fluorescent dye within the polystyrene matrix. During this step Tween, a nonionic surfactant, is added to stabilize the particles as the charge stabilization is not functioning in an organic environment. It seems that this Tween is then not properly washed away after the procedure.

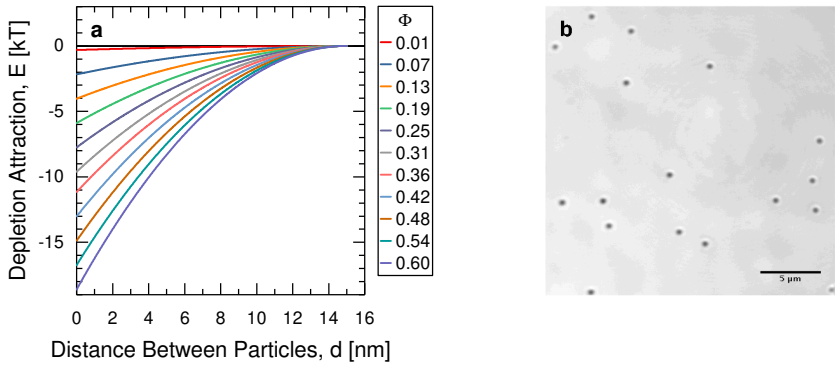

Figure 6.5: a: Theoretical strength of the depletion attraction between two particles at different volume fractions of α-crystallin. **b:** Microscope image of particles after incubation in a solution of α-crystallin. The bar represents a length of 5 µm.

The presence of Tween appeared to prevent the pegylation, most likely by physically restricting PEG from accessing the carboxyl groups on the particle surface. Successful surface functionalization was achieved by prewashing the particles using dialysis against H_2O before the treatment. The presence of Tween actually made the untreated particles stable in a high ionic solvent, something that should not be possible for electrostatically stabilized particles. However, this effect was lost after washing as expected.

6.1.3 Depletion Interaction

One serious cause of concern with microrheology of protein systems in general is the possibility of depletion interactions leading to particle association, described in section 5.2 as well as more thoroughly in Paper I and the accompanying supporting information. Figure 6.5a shows the calculated strength of this attractive potential at different protein concentrations from equation 5.2, assuming naked hard sphere particles. The theoretical samples consist of α-crystallin chosen due to its relatively large size resulting in an extended range of the attraction compared to smaller proteins. From this, it was clear that depletion interactions may play a significant role in the current system.

Now, the difference between this theoretical scenario and the actual case is that the particles are coated with a layer of PEG. This complicates the model significantly and there does not appear to exist a consensus in literature on how such a layer will affect the interaction potential, with some even suggesting a stabilization effect opposing the depletion attraction.[172,186,187] It proved to be difficult to 100% verify the presence of depletion or lack thereof in the current system. The way that was conceived was to

disperse particles in a sample of α-crystallin and wait several hours before performing visual inspection using microscopy which displayed no indications of aggregates, example image in figure 6.5b. There have also been no signs of any apparent size increase as measured with DLS over time in samples which also indicates that depletion does not have an impact on the system. It is still not clear as to why there is no apparent sign of aggregation due to depletion attraction. It could be due to the aforementioned stabilization effect or it could be that the particle concentration is just low enough that it is not kinetically reasonable for aggregation to occur over the time frame of the experiments.

6.2 Proteins

6.2.1 Lysozyme

Lysozyme is, together with entities such as BSA, one of the most well studied protein systems. As such, it served as a good verification system for the reliability of the microrheology method, as detailed in Paper I, especially since its viscosity-concentration profile at 5°C was already available in literature.[11] These experiments were performed at minimal ionic strength so as to not screen any long range electrostatic interactions. This was to get a situation where the combination of SALR, described in section 2.1.1, caused the formation of equilibrium clusters.[11] Figure 6.6a shows these two data sets agreeing over the entire concentration range after the density corrections discussed in section 2.3. One thing to especially note is the sparse number of data points at low concentrations available from literature, which was caused by the need for extrapolation from high-shear measurements and thus made the determination of low viscosities difficult.[14]

It is possible to determine an effective volume fraction of the protein samples using equation 3.2, assuming the Quemada relation holds for the system as discussed in section 3.3. The fit used to retrieve the conversion factor ($\Phi_{max}{}^{theory}/\Phi_{max}{}^{measured} = 2.27$) from the microrheology data is shown in figure 6.6b with the final viscosity plot in figure 6.6c together with the corresponding Quemada relation. The conversion factor is close to the 2.22 which was previously reported in literature,[11] which supports the picture that electrostatic repulsion between the charged clusters drives the arrest transition.

The experiments so far have demonstrated the viability of DLS-microrheology to yield the same viscosities as those from rheometry over a wide concentration range. However, no measurements have been possible of volume fractions at and beyond Φ_{max}. This is mainly due to two reasons, first it's difficult to prepare sufficient volumes with high

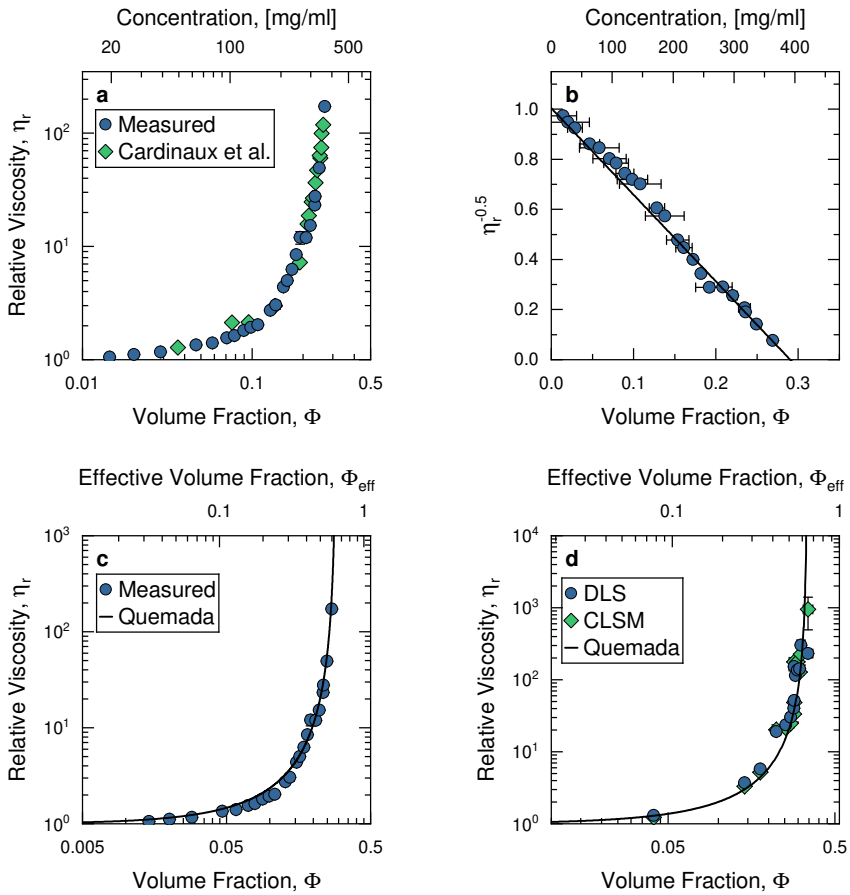

Figure 6.6: a: Viscosity of lysozyme solutions at 5°C determined using microrheology and compared to rheometer-based values found in literature.[11] **b:** The plot to determine Φ_{max} of the system which is then used to calculate Φ_{eff} from equation 3.2. **c:** The measured viscosities with the effective volume fractions together with the Quemada-relation for $\Phi_{max} = 0.64$. **d:** The viscosity of lysozyme at 20°C as measured with both CLSM and DLS showing that both methods yield the same result. The effective volume fraction was calculated and the viscosity behavior shown to follow the Quemada relation.

concentrations using the Amicon procedure since the final increases are very minor and the centrifugations mainly result in concentration gradients occurring in the tube. The second comes from the fact that the addition of particles leads to a minor dilution of the sample which at high protein concentrations is not insignificant. Lysozyme was chosen as the test protein in an effort to push the sample concentrations as high as possible. This was due to its high availability and relatively easy preparation procedure but also from the contradicting results in literature whether an arrest transition truly exists for the system.[11,12,105]

This project is detailed in Paper III and the primary idea was to utilize CLSM to perform

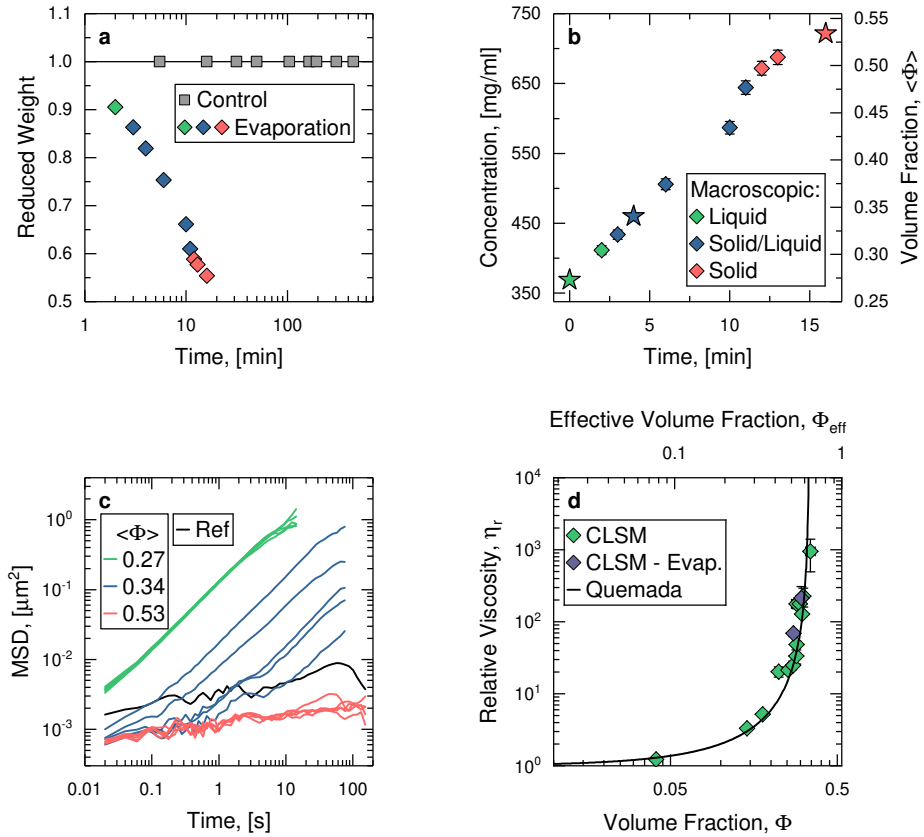

Figure 6.7: The evaporation method allowed reaching concentrations not available using conventional means. **a:** The diamonds show the change in weight of the sample, demonstrating a relatively rapid decrease. A reference which was immediately sealed, grey squares, showed no change even after several hours. **b:** The sample concentration calculated from the change in weight, color coded after the macroscopic behavior observed during sealing. **c:** Examples of MSD:s from the points marked as stars in figure **b** showing the span from liquid to solid behavior via an intermediate heterogeneous state. **d:** Comparison of the viscosity obtained from evaporation samples showing fluid behavior with those prepared by conventional means.

MPT, described in section 5.5, as this would require much smaller volumes (~ 5 µl) as compared to DLS (~ 100 µl) and it should thus be possible to more easily prepare highly concentrated samples. The first thing was to extend the particle preparation to fluorescent particles as described further in section 6.1.2. A set of samples were prepared with 0.2 µm particles and measured at 20°C to confirm that the result obtained from CLSM corresponds to those measured with DLS. The results, displayed in figure 6.6d, shows great overlap for all but one of the most concentrated samples. The effective volume fraction is determined the same way as previously described in figure 6.6b/c but with a conversion factor of 1.89 from equation 3.2 instead.

Despite the reduction in sample volume it was not enough to reach the arrested region due to the step of adding particles. A way was derived to reach these high concentrations based on evaporation as described in section 5.5.2 and Paper III. Figure 6.7a shows the change in weight of the experimental setup which shows linearity with time until extremely high concentrations were reached. A control consisting of an immediately sealed sample cell was continuously measured for several hours showing that, once sealed, there is no change in sample concentration at least during the extent of the experiments.

During the sealing of the sample cells it was noted that the sample behaved macroscopically different depending on the duration of evaporation. This is displayed in figure 6.7b, which also contains the estimated final average volume fraction of the evaporated samples based on the amount of solvent that disappeared. Initially the samples easily flow when sealed, indicated with green points. However, after some time there seems to be a more heterogeneous distribution, shown as blue points, with a more concentrated outer region and a more liquid-like core that is becoming more homogenized during the sealing process. Finally, the sample does not show such a visible heterogeneity and is actually quite difficult to properly seal due to the solidity of the sample, displayed as red points.

Figure 6.7c shows MSD:s recorded at several different locations within the samples denoted as stars in figure 6.7b, with a black line showing the noise floor inherent in measurements due to instrumental drift. For the lower concentration there is full overlap at the different regions within the sample displaying fluid behavior, then around the arrest transition there is clearly more heterogeneity with some regions being more fluid- or more solid-like. Finally, the measurements overlap again once every location investigated within the sample display a fully arrested state.

Figure 6.7d shows the viscosity data from MPT in figure 6.6d together with viscosities retrieved from the evaporation samples that displayed viscous behaviour. This verifies that samples prepared with the evaporation method yields the same result as conventionally prepared samples.

6.2.2 α-crystallin

The protein α-crystallin is a vital part to maintain a healthy environment in the eye lens due to its chaperone activity, as described in section 2.1.2. It appears to also be the only crystallin that has had its entire viscosity-concentration dependency detailed using rheometry. [27] There it was shown to follow the behaviour of a classic hard sphere system at physiological buffer conditions. It was therefor a suitable system to act as a second verification of the microrheology methodology together with lysozyme, described in

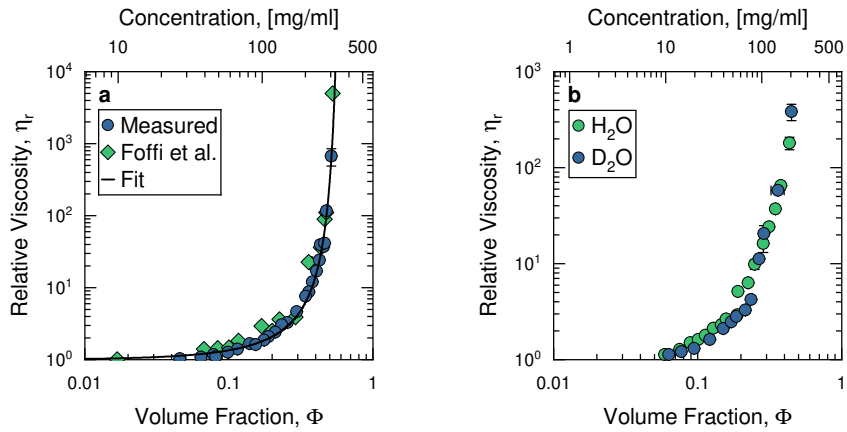

Figure 6.8: a: Viscosity of α-crystallin measured using microrheology and compared to rheometer based results in literature.[27] The fit is to the Mooney relation and yields fitted parameters agreeing with those expected for a hard sphere system. **b:** Viscosity of β_H-crystallin in H_2O and D_2O conditions showing that the microrheology methodology is valid also in D_2O-based samples.

section 6.2.1, and further detailed in Paper I. There is clearly an agreement between the two data sets, as shown in figure 6.8a, thus further confirming the viability of the microrheology method.

The best fit to the microrheology data was obtained using the Mooney relation, equation 3.1b described further in section 3.2. This yielded values for the fitted parameters of $[\eta] = 2.55$ and $\Phi_{max} = 0.646$ which are very close to the values expected for a system with hard sphere interactions, $[\eta] = 2.5$ and $\Phi_{max} = 0.64$. Thus confirming that α-crystallin indeed behaves as hard spheres at these conditions.

6.2.3 β_H-crystallin

General investigations of systems such as proteins often involve the use of neutron-based scattering techniques. One such technique, called neutron spin echo, can be used to investigate concentrated systems to illuminate how interactions between proteins influences the short-time dynamics. In order to successfully utilize neutron scattering techniques, it is often necessary to use D_2O instead of H_2O to minimize incoherent background. It was therefor necessary to investigate if the microrheology methodology with the current tracer particles were operational also in a D_2O-system. The protein chosen for this was β_H-crystallin as it will also be needed for comparison with neutron data in later publications focused on this protein. Despite being an eye-lens protein, it has received relatively little scientific interest. This is most likely due to it not having been shown to possess neither an interesting interaction scheme such as that of γ_B-

crystallin nor having a direct influence on lens health with a chaperone effect like that of α-crystallin.

Figure 6.8b shows two sets of experiments with β-crystallin in either H_2O- or D_2O-based phosphate buffer. There is some minor deviation between the two data sets at the intermediate concentrations but the overall trend, especially when approaching the arrest transition, appears to be consistent between the the two solvents. In contrast to the results from α-crystallin, it was not possible to directly fit this data to models for hard spheres. The reason for this is currently not clear, but could be due to the suggested significant polydispersity of the system[29] or some currently unknown interaction potential.

6.2.4 γ_B-crystallin

The interactions of γ-crystallin is believed to be of high importance to achieve and maintain the high protein concentration within the eye lens, as further described in section 2.1.2. As previously noted, the work in this thesis has exclusively been on the subtype γ_B-crystallin. Its rheological properties have never been studied previously due to the extremely time and resource demanding procedure of acquiring the protein detailed in section 2.2.2. This project is further detailed and discussed in Paper IV.

The critical concentration and temperature are known to occur around $\Phi_c = 0.15$ and $T_c = 19°C$ for this system.[42] First of all, microrheology measurements were performed at four different temperatures ($T = 20; 25; 30; 35°C$) which range from far away to within close vicinity of the critical temperature. The temperature will influence the apparent strength of the attractive interactions between the proteins. The existence of a critical region proved to cause major problems for the DLS-based microrheology method. This was due to a substantial increase in protein scattering as well as a significant overlap between the particle and protein decays which made it difficult to extract reliable data originating from the tracer particles as detailed in Paper IV.

Figure 6.9 shows the results obtained from both DLS and MPT for the four different temperatures. There is a suspicious local increase in the apparent viscosity from the DLS measurements around the critical concentration, Φ_c. The origin of this is not fully understood but it could be due to the difficulty in fitting the data or it could have a more complicated origin such as critical Casimir forces.[188] For this reason, the MPT was performed using untreated 0.5 µm particles which fortunately agreed with the DLS results over the entire range except around the critical concentration. This indicates that scattering based microrheology around or close to critical regions of a system is inherently problematic.

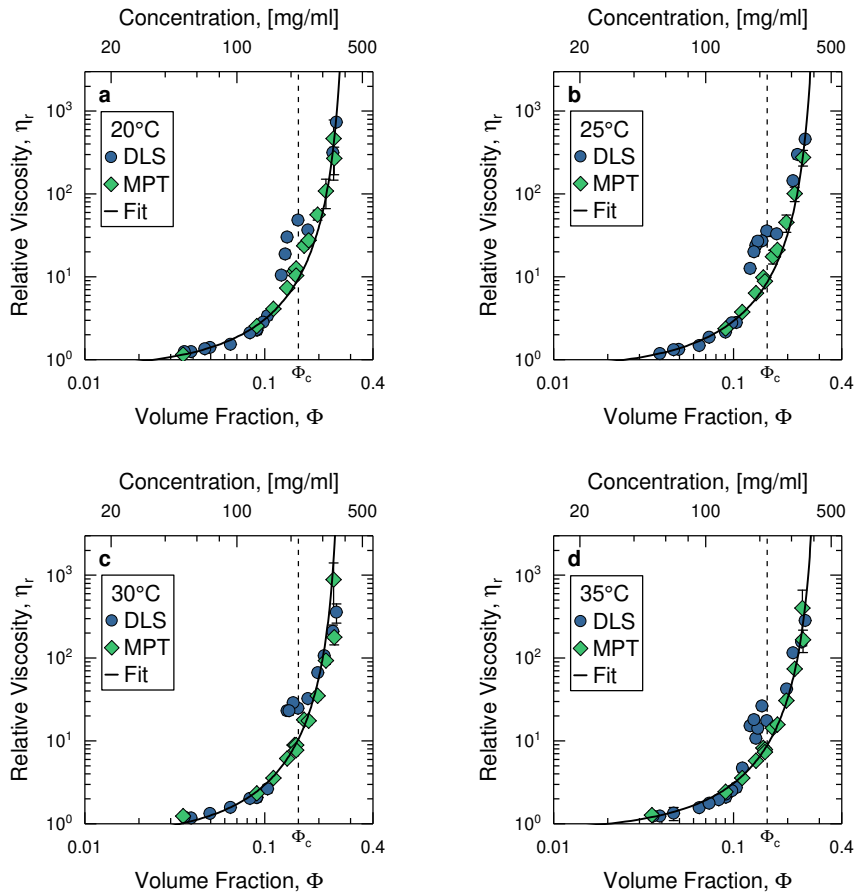

Figure 6.9: Viscosity of γ_B at four different temperatures (**a:** 20°C **b:** 25°C **c:** 30°C **d:** 35°C) determined using DLS- and MPT-based microrheology. This revealed a problem with the DLS measurements around Φ_c which was not reproducible using MPT. The fits were obtained using equation 3.3 with $\nu = 3.23$ and appears to describe the data sets well over the concentration range.

The best fit to the data was using the attractive model described in section 3.3 and equation 3.3 using a value of $\nu = 3.23$.[93] There was no apparent difference in the value of Φ_{max}, varying between 0.27-0.29, for the four different temperatures. This was confirmed using the evaporation method to create samples beyond the arrest transition akin to those described in section 6.2.1 for lysozyme. Normalizing the viscosities at the different temperatures against T = 35°C for the MPT data, shown in figure 6.10, reveals some temperature dependence where the viscosity increases with reduced temperature. So even though the changes in interactions does not appear to influence the location of the arrest it does affect the viscosity of the system leading up to those concentrations.

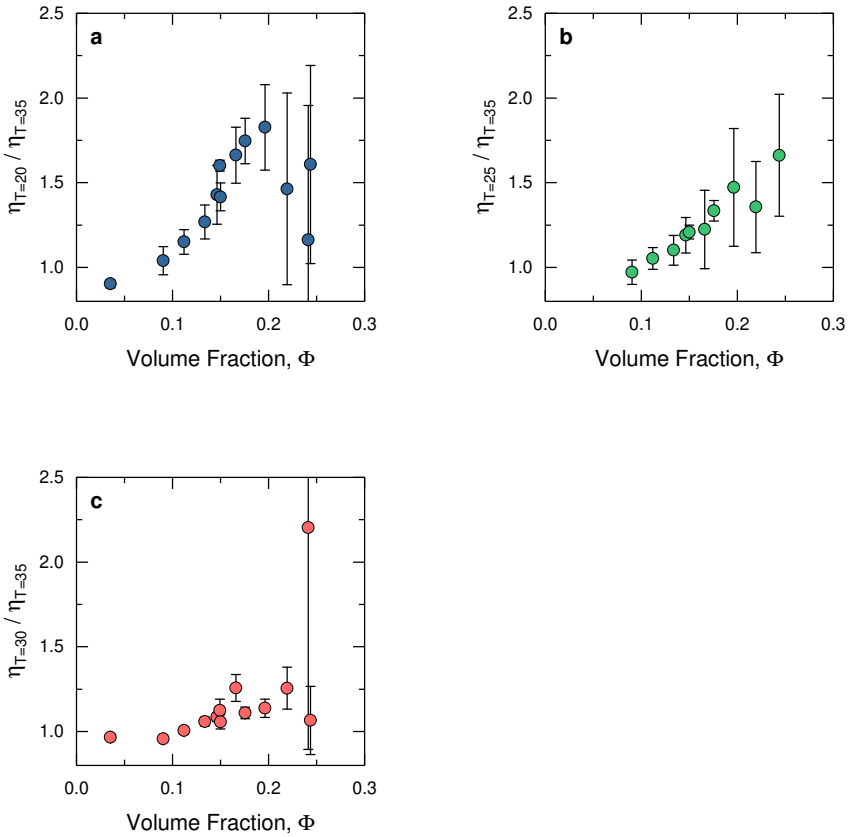

Figure 6.10: The change in viscosity with temperature compared to T = 35°C, showing an increase when approaching T_c. **a:** 20°C **b:** 25°C **c:** 30°C

They asked me how well I understood theoretical physics.
I said I had a theoretical degree in physics.
They said welcome aboard.
— Fantastic, F:NV

CHAPTER 7

CONCLUSIONS & OUTLOOK

This work has focused on establishing an experimental procedure to investigate the zero shear viscosity of concentrated protein solutions close to the arrest transition. The behavior of this type of concentrated system is of high interest for several reasons. Not only is it directly related to certain biological functions such as that of the eye lens but also in regards to protein condensation diseases as well as the use of concentrated protein biologics.

A tailored tracer particle was developed and shown to perform well in the presence of proteins in different buffers. A method to investigate the viscosity-concentration dependency using DLS-based microrheology was conceived using a specialized 3D-DLS technique to suppress multiple scattering. It was then applied to different protein systems, such as certain eye-lens crystallins that had never been rheologically investigated before due to the limited supply of protein. This method worked well for every protein system tested except around the critical region displayed by γ_B-crystallin where the protein scattering became too significant.

The tracer system was adjusted to work with fluorescent particles which made it possible to perform microscopy-based microrheology. This method made it viable to investigate protein systems close to the critical region where DLS failed. A secondary sample preparation approach involving evaporation to further concentrate samples allowed the arrest transition to be reached and surpassed. This made it possible to confirm the location of the arrest transition directly, something that otherwise is extrapolated from measurements of less concentrated samples.

Future opportunities with this tracer particle system and the microrheology methodology can involve more complex systems such as mixtures of different proteins. This is of particular interest for the eye lens system where the combination of the different

proteins at high concentrations creates a unique biological system. Another type of sample that may be of interest for this methodology can be that which have a temporal component where the viscosity evolves over time. Microrheology can allow for non-invasive measurements of the same sample over a vast time-span in contrast to other rheological methods where aliquots need to be extracted at different time points. A more exotic reason focused on fundamental science is for example the investigation of depletion interaction and how it depends on surface coating. Changing the size of the attached PEG as well as varying the solvent quality can make it possible to experimentally investigate depletion attraction between particles where the interaction is not truly hard sphere like.

REFERENCES

[1] Cravatt, B. F., Wright, A. T. & Kozarich, J. W. Activity-Based Protein Profiling: From Enzyme Chemistry to Proteomic Chemistry. *Annual Review of Biochemistry* 77, 383–414 (2008).

[2] Wang, W., Singh, S., Zeng, D. L., King, K. & Nema, S. Antibody Structure Instability, and Formulation. *Journal of Pharmaceutical Sciences* **96**, 1–26 (2007).

[3] Dominguez, R. & Holmes, K. C. Actin Structure and Function. *Annual Review of Biophysics* **40**, 169–186 (2011).

[4] Sweeney, P., Park, H., Baumann, M., Dunlop, J., Frydman, J., Kopito, R., McCampbell, A., Leblanc, G., Venkateswaran, A., Nurmi, A. & Hodgson, R. Protein Misfolding in Neurodegenerative Diseases: Implications and Strategies. *Translational Neurodegeneration* **6:6** (2017).

[5] Feder, M. E. & Hofmann, G. E. Heat-shock Proteins Molecular Chaperones, and the Stress Response: Evolutionary and Ecological Physiology. *Annual Reviews of Physiology* **61**, 243–282 (1999).

[6] Broide, M. L., Tominc, T. M. & Saxowsky, M. D. Using Phase Transitions to Investigate the Effect of Salts on Protein Interactions. *Physical Review E* **53**, 6325–6335 (1996).

[7] Board, R. G. Review Article: The Course of Microbial Infection of the Hens Egg. *Journal of Applied Bacteriology* **29**, 319–341 (1966).

[8] Stradner, A., Sedgwick, H., Cardinaux, F., Poon, W. C. K., Egelhaaf, S. U. & Schurtenberger, P. Equilibrium Cluster Formation in Concentrated Protein Solutions and Colloids. *Nature* **432**, 492–495 (2004).

[9] Chiti, F. & Dobson, C. M. Protein Misfolding Functional Amyloid, and Human Disease. *Annual Review of Biochemistry* **75**, 333–366 (2006).

[10] Moreau, K. L. & King, J. A. Protein Misfolding and Aggregation in Cataract Disease and Prospects for Prevention. *Trends in Molecular Medicine* **18**, 273–282 (2012).

[11] Cardinaux, F., Zaccarelli, E., Stradner, A., Bucciarelli, S., Farago, B., Egelhaaf, S. U., Sciortino, F. & Schurtenberger, P. Cluster-Driven Dynamical Arrest in Concentrated Lysozyme Solutions. *The Journal of Physical Chemistry B* **115**, 7227–7237 (2011).

[12] Godfrin, P. D., Hudson, S. D., Hong, K., Porcar, L., Falus, P., Wagner, N. J. & Liu, Y. Short-Time Glassy Dynamics in Viscous Protein Solutions with Competing Interactions. *Physical Review Letters* **115**, 228302 (2015).

[13] Allan, D. B., Firester, D. M., Allard, V. P., Reich, D. H., Stebe, K. J. & Leheny, R. L. Linear and Nonlinear Microrheology of Lysozyme Layers Forming at the Air-water Interface. *Soft Matter* **10**, 7051–7060 (2014).

[14] Cardinaux, F., Zaccarelli, E., Stradner, A., Bucciarelli, S., Farago, B., Egelhaaf, S. U., Sciortino, F. & Schurtenberger, P. Supporting Information: Cluster-Driven Dynamical Arrest in Concentrated Lysozyme Solutions. *J. Phys. Chem. B* **115**, 7227–7237 (2011).

[15] Shoichet, K., Baase, W. A., Kuroki, R. & Matthews, B. W. A Relationship Between Protein Stability and Protein Function. *Proceedings of the National Academy of Sciences* **92**, 452–456 (1995).

[16] Andley, U. P. Crystallins in the Eye: Function and Pathology. *Progress in Retinal and Eye Research* **26**, 78–98 (2007).

[17] Krause, A. C. Chemistry of the Lens I. Composition of Albuminoid and Alpha Crystallin. *Arch Ophthalmol.* **8**, 166–172 (1932).

[18] de Jong, W. W., Lubsen, N. H. & Kraft, H. J. Molecular Evolution of the Eye Lens. *Progress in Retinal and Eye Research* **13**, 391–442 (1994).

[19] Delaye, M. & Tardieu, A. Short-range Order of Crystallin Proteins Accounts for Eye Lens Transparency. *Nature* **302**, 415–417 (1983).

[20] Wride, M. A. Lens Fibre Cell Differentiation and Organelle Loss: Many Paths Lead to Clarity. *Philosophical Transactions of the Royal Society B: Biological Sciences* **366**, 1219–1233 (2011).

[21] Bassnett, S., Shi, Y. & Vrensen, G. F. J. M. Biological Glass: Structural Determinants of Eye Lens Transparency. *Philosophical Transactions of the Royal Society B: Biological Sciences* **366**, 1250–1264 (2011).

[22] Wistow, G. J. & Piatigorsky, J. Lens Crystallins: The Evolution and Expression of Proteins for a Highly Specialized Tissue. *Annual Review of Biochemistry* **57**, 479–504 (1988).

[23] Slingsby, C. & Clout, N. J. Structure of the Crystallins. *Eye (London, England)* **13**, 395–402 (1999).

[24] Bloemendal, H., de Jong, W., Jaenicke, R., Lubsen, N. H., Slingsby, C. & Tardieu, A. Ageing and Vision: Structure, Stability and Function of Lens Crystallins. *Progress in Biophysics and Molecular Biology* **86**, 407–485 (2004).

[25] Truscott, R. J. W. Eye Lens Proteins and Cataracts. In Uversky, V. N. & Fink, A. (eds.) *Protein Misfolding, Aggregation, and Conformational Diseases Part B: Molecular Mechanisms of Conformational Diseases*, chap. 21, 435–447 (Springer, New York, 2007), 1 edn.

[26] Horwitz, J. α-Crystallin can Function as a Molecular Chaperone. *Proceedings of the National Academy of Sciences of the United States of America* **89**, 10449–10453 (1992).

[27] Foffi, G., Savin, G., Bucciarelli, S., Dorsaz, N., Thurston, G. M., Stradner, A. & Schurtenberger, P. Hard Sphere-like Glass Transition in Eye Lens α-Crystallin Solutions. *Proceedings of the National Academy of Sciences of the United States of America* **111**, 16748–16753 (2014).

[28] Slingsby, C. & Bateman, O. A. Quaternary Interactions in Eye Lens β-Crystallins: Basic and Acidic Subunits of β-Crystallins Favor Heterologous Association. *Biochemistry* **29**, 6592–6599 (1990).

[29] Tardieu, A., Veretout, F., Krop, B. & Slingsby, C. Protein Interactions in the Calf Eye Lens: Interactions Between β-Crystallins Are Repulsive Whereas in γ-Crystallins They Are Attractive. *Eur. Phys. J.* **21**, 1–12 (1992).

[30] Nostrand, K. P. V., Michel, L. V., Lampi, K. J. & Thurston, G. M. Static and Quasielastic Light Scattering Studies of Bovine βH Crystallin. *Working Paper* (2017).

[31] Kumaraswamy, V. S., Lindley, P. F., Slingsby, C. & Glover, I. D. An Eye Lens Protein-water Structure: 1.2 Å Resolution Structure of γB-crystallin at 150 K. *Acta Crystallographica Section D: Structural Biology* **D52**, 611–622 (1996).

[32] Najmudin, S., Nalini, V., Driessen, H. P. C., Slingsby, C., Blundell, T. L., Moss, D. S. & Lindley, P. F. Structure of the Bovine Eye Lens Protein γB (γII)-Crystallin at 1.47 Å. *Acta Crystallographica Section D: Structural Biology* **D49**, 223–233 (1993).

[33] Jones, C. E., Atchison, D. A., Meder, R. & Pope, J. M. Refractive Index Distribution and Optical Properties of the Isolated Human Lens Measured Using Magnetic Resonance Imaging (MRI). *Vision Research* **45**, 2352–2366 (2005).

[34] Moffat, B. A., Atchison, D. A. & Pope, J. M. Explanation of the Lens Paradox. *Optometry and Vision Science* **79**, 148–150 (2002).

[35] Greiling, T. M. S. & Clark, J. I. New Insights into the Mechanism of Lens Development Using Zebra Fish. In Jeon, K. W. (ed.) *International Review of Cell and Molecular Biology*, vol. 296, chap. 1, 1–61 (Elsevier Inc., 2012), 1 edn.

[36] Zhao, H., Chen, Y., Rezabkova, L., Wu, Z., Wistow, G. & Schuck, P. Solution Properties of γ-Crystallins: Hydration of Fish and Mammal γ-Crystallins. *Protein Science* **23**, 88–99 (2014).

[37] Héon, E., Priston, M., Schorderet, D. F., Billingsley, G. D., Girard, P. O., Lubsen, N. & Munier, F. L. The γ-Crystallins and Human Cataracts: A Puzzle Made Clearer. *American journal of human genetics* **65**, 1261–1267 (1999).

[38] Pande, A., Pande, J., Asherie, N., Lomakin, A., Ogun, O., King, J. & Benedek, G. B. Crystal Cataracts: Human Genetic Cataract Caused by Protein Crystallization. *Proceedings of the National Academy of Sciences of the United States of America* **98**, 6116–6120 (2001).

[39] Stradner, A., Thurston, G. M. & Schurtenberger, P. Tuning Short-range Attractions in Protein Solutions: From Attractive Glasses to Equilibrium Clusters. *Journal of Physics Condensed Matter* **17**, S2805–S2816 (2005).

[40] Stradner, A., Foffi, G., Dorsaz, N., Thurston, G. & Schurtenberger, P. New Insight into Cataract Formation: Enhanced Stability through Mutual Attraction. *Physical Review Letters* **99**, 198103 (2007).

[41] Dorsaz, N., Thurston, G. M., Stradner, A., Schurtenberger, P. & Foffi, G. Phase Separation in Binary Eye Lens Protein Mixtures. *Soft Matter* **7**, 1763–1776 (2011).

[42] Bucciarelli, S., Casal-Dujat, L., De Michele, C., Sciortino, F., Dhont, J., Bergenholtz, J., Farago, B., Schurtenberger, P. & Stradner, A. Unusual Dynamics of Concentration Fluctuations in Solutions of Weakly Attractive Globular Proteins. *Journal of Physical Chemistry Letters* **6**, 4470–4474 (2015).

[43] Lindenmann, J. Origin of the Terms 'Antibody' and 'Antigen'. *Scandinavian Journal of Immunology* **19**, 281–285 (1984).

[44] Carter, P. Improving the Efficacy of Antibody-Based Cancer Therapies. *Nature Reviews Cancer* **1**, 118–129 (2001).

[45] Burckbuchler, V., Mekhloufi, G., Giteau, A. P., Grossiord, J. L., Huille, S. & Agnely, F. Rheological and Syringeability Properties of Highly Concentrated Human Polyclonal Immunoglobulin Solutions. *European Journal of Pharmaceutics and Biopharmaceutics* **76**, 351–356 (2010).

[46] Shire, S. J., Shahrokh, Z. & Liu, J. Challenges in the Development of High Protein Concentration Formulations. *Journal of Pharmaceutical Sciences* **93**, 1390–1402 (2004).

[47] Good, N. E., Winget, G. D., Winter, W., Connolly, T. N., Izawa, S. & Sing, R. M. M. Hydrogen Ion Buffers for Biological Research. *Biochemistry* **5**, 467–477 (1966).

[48] Kapitza, P. Viscosity of Liquid Helium Below the λ-Point. *Nature* **141**, 74 (1938).

[49] Allen, J. F. & Misener, A. D. Flow of Liquid Helium II. *Nature* **141**, 75 (1938).

[50] Simon, F. E. & Swenson, C. A. The Liquid-Solid Transition in Helium near Absolute Zero. *Nature* **165**, 829–831 (1950).

[51] Leggett, A. J. Can a Solid be "Superfluid"? *Physical Review Letters* **25**, 1543–1546 (1970).

[52] Edgeworth, R., Dalton, B. J. & Parnell, T. The Pitch Drop Experiment. *European Journal of Physics* **5**, 198–200 (1984).

[53] White, A. After 13 years, progress in pitch-drop experiment (w/ video) (2014, April 17); https://phys.org/news/2014-04-years-pitch-drop.html; Accessed: 2018-12-04.

[54] Anton Paar Online Article Repository; https://wiki.anton-paar.com/en/articles/; Accessed: 2018-12-04.

[55] Mezger, T. G. *The Rheology Handbook 3rd Revised Edition* (Vincentz Network GmbH & Co KG, Hanover, Germany, 2011), 3 edn.

[56] Atkins, P. & de Paula, J. *Atkins Physical Chemistry* (Oxford University Press, Oxford, UK, 2006), 8 edn.

[57] Findlay, A. & Kitchener, J. A. *Findlayss Practical Physical Chemistry* (William Clowes and Sons, London, 1967), 8 edn.

[58] Rutgers, I. R. Relative Viscosity and Concentration. *Rheologica Acta* **2**, 305–348 (1962).

[59] Dörr, A., Sadiki, A. & Mehdizadeh, A. A Discrete Model for the Apparent Viscosity of Polydisperse Suspensions Including Maximum Packing Fraction. *Journal of Rheology* **57**, 743–765 (2013).

[60] Pusey, P. N., van Megen, W., Underwood, S. M., Bartlett, P. & Ottewill, R. H. Colloidal Fluids, Crystals and Glasses. *Physica A: Statistical Mechanics and its Applications* **176**, 16–27 (1991).

[61] Sciortino, F. & Tartaglia, P. Glassy Colloidal Systems. *Advances in Physics* **54**, 471–524 (2005).

[62] Sciortino, F. Disordered Materials: One Liquid, Two Glasses. *Nature materials* **1**, 145–146 (2002).

[63] Pham, K. N., Egelhaaf, S. U., Pusey, P. N. & Poon, W. C. K. Glasses in Hard Spheres with Short-Range Attraction. *Physical Review E* **69**, 011503 (2004).

[64] Poon, W. C. Colloidal Glasses. *MRS Bulletin* **29**, 96–99 (2004).

[65] Pusey, P. N. & van Megen, W. Phase Behaviour of Concentrated Suspensions of Nearly Hard Colloidal Spheres. *Nature* **320**, 340–342 (1986).

[66] Pusey, P. N. & van Megen, W. Observation of a Glass Transition in Suspensions of Spherical Colloidal Particles. *Physical Review Letters* **59**, 2083–2086 (1987).

[67] van Megen, W. & Underwood, S. M. Glass Transition in Colloidal Hard Spheres: Measurement and Mode-Coupling-Theory Analysis of the Coherent Intermediate Scattering Function. *Physical Review E* **49**, 4206–4220 (1994).

[68] Marshall, L. & Zukoski IV, C. F. Experimental Studies on the Rheology of Hard-Sphere Suspensions near the Glass Transition. *Journal of Physical Chemistry* **94**, 1164–1171 (1990).

[69] Cheng, Z., Zhu, J., Chaikin, P. M., Phan, S. E. & Russel, W. B. Nature of the Divergence in Low Shear Viscosity of Colloidal Hard-sphere Dispersions. *Physical Review E* **65**, 041405 (2002).

[70] Hunter, G. L. & Weeks, E. R. The Physics of the Colloidal Glass Transition. *Reports on Progress in Physics* **75**, 066501 (2012).

[71] Dawson, K. A. The Glass Paradigm for Colloidal Glasses, Gels, and Other Arrested States Driven by Attractive Interactions. *Current Opinion in Colloid and Interface Science* **7**, 218–227 (2002).

[72] Trappe, V. & Sandkühler, P. Colloidal Gels - Low-Density Disordered Solid-Like States. *Current Opinion in Colloid and Interface Science* **8**, 494–500 (2004).

[73] Cipelletti, L. & Ramos, L. Slow Dynamics in Glassy Soft Matter. *Journal of Physics Condensed Matter* **17**, R253–R285 (2005).

[74] Poon, W. C. K., Weeks, E. R. & Royall, C. P. On Measuring Colloidal Volume Fractions. *Soft Matter* **8**, 21–30 (2012).

[75] Royall, C. P. & Williams, S. R. The Role of Local Structure in Dynamical Arrest. *Physics Reports* **560**, 1–75 (2015).

[76] Golde, S., Palberg, T. & Schöpe, H. J. Supporting Information: Correlation Between Dynamical and Structural Heterogeneities in Colloidal Hard-Sphere Suspensions. *Nature Physics* **12**, 712–717 (2016).

[77] Meeker, S. P., Poon, W. C. K. & Pusey, P. N. Concentration Dependence of the Low-shear Viscosity of Suspensions of Hard-Sphere Colloids. *Physical Review E* **55**, 5718–5722 (1997).

[78] Joshi, Y. M. Dynamics of Colloidal Glasses and Gels. *Annual Review of Chemical and Biomolecular Engineering* **5**, 181–202 (2014).

[79] Einstein, A. Eine neue Bestimmung der Moleküldimensionen. *Annalen der Physik* **19**, 289–306 (1906).

[80] Eilers, V. H. Die Viskosität von Emulsionen hochviskoser Stoffe als Funktion der Konzentration. *Kolloid-Zeitschrift* **97**, 313–321 (1941).

[81] Mendoza, C. I. & Santamaría-Holek, I. The Rheology of Hard Sphere Suspensions at Arbitrary Volume Fractions: An Improved Differential Viscosity Model. *Journal of Chemical Physics* **130**, 044904 (2009).

[82] Bernal, J. D. The Structure of Liquids. *Scientific American* **203**, 124–137 (1960).

[83] Bernal, J. D. The Structure of Liquids. *The Bakerian Lecture* (1962).

[84] Bernal, J. D. & Mason, J. Packing of Spheres: Co-Ordination of Randomly Packed Spheres. *Nature* **188**, 910–911 (1960).

[85] Finney, J. L. Bernal's Road to Random Packing and the Structure of Liquids. *Philosophical Magazine* **93**, 3940–3969 (2013).

[86] Mooney, M. The Viscosity of a Concentrated Suspension of Spherical Particles. *J. Colloid and Interface Science* **6**, 162–170 (1951).

[87] Krieger, I. M. & Dougherty, T. J. A Mechanism for Non-Newtonian Flow in Suspensions of Rigid Spheres. *Transactions of The Society of Rheology* **3**, 137–152 (1959).

[88] Quemada, D. Rheology of Concentrated Disperse Systems and Minimum Energy Dissipation Principle - I. Viscosity-Concentration Relationship. *Rheologica Acta* **16**, 82–94 (1977).

[89] Horn, F. M., Richtering, W., Bergenholtz, J., Willenbacher, N. & Wagner, N. J. Hydrodynamic and Colloidal Interactions in Concentrated Charge-Stabilized Polymer Dispersions. *Journal of Colloid and Interface Science* **225**, 166–178 (2000).

[90] Willenbacher, N. & Georgieva, K. Rheology of Disperse Systems. In Bröckel, U., Meier, W. & Wagner, G. (eds.) *Product Design and Engineering: Formulation of Gels and Pastes*, chap. 1, 7 – 49 (Wiley VCH Verlag GmbH & Co, Singapore, 2013), 1 edn.

[91] Zaccarelli, E., Foffi, G., Dawson, K. A., Buldyrev, S. V., Sciortino, F. & Tartaglia, P. Confirmation of Anomalous Dynamical Arrest in Attractive Colloids: A Molecular Dynamics Study. *Physical Review E* **66**, 041402 (2002).

[92] Sciortino, F., Tartaglia, P. & Zaccarelli, E. Evidence of a Higher-order Singularity in Dense Short-Ranged Attractive Colloids. *Physical Review Letters* **91**, 268301 (2003).

[93] Puertas, A. M., de Michele, C., Sciortino, F., Tartaglia, P. & Zaccarelli, E. Viscoelasticity and Stokes-einstein Relation in Repulsive and Attractive Colloidal Glasses. *Journal of Chemical Physics* **127**, 144906 (2007). 0705.2988.

[94] Fabbian, L., Götze, W., Sciortino, F., Tartaglia, P. & Thiery, F. Ideal Glass-Glass Transitions and Logarithmic Decay of Correlations in a Simple System. *Physical Review E* **59**, R3147–R1350 (1999).

[95] Bergenholtz, J. & Fuchs, M. Nonergodicity Transitions in Colloidal Suspensions with Attractive Interactions. *Physical Review E* **59**, 5706–5715 (1999).

[96] Mallamace, F., Gambadauro, P., Micali, N., Tartaglia, P., Liao, C. & Chen, S. H. Kinetic Glass Transition in a Micellar System with Short-Range Attractive Interaction. *Physical Review Letters* **84**, 5431–5434 (2000).

[97] Pham, K. N., Puertas, A. M., Bergenholtz, J., Egelhaaf, S. U., Moussaïd, A., Pusey, P. N., Schofield, A. B., Cates, M. E., Fuchs, M. & Poon, W. C. K. Multiple Glassy States in a Simple Model System. *Science* **296**, 104–106 (2002).

[98] Eckert, T. & Bartsch, E. Re-entrant Glass Transition in a Colloid-Polymer Mixture with Depletion Attractions. *Physical Review Letters* **89**, 125701 (2002).

[99] Chen, W. R., Chen, S. H. & Mallamace, F. Small-angle Neutron Scattering Study of the Temperature-Dependent Attractive Interaction in Dense L64 Copolymer Micellar Solutions and Its Relation to Kinetic Glass Transition. *Physical Review E* **66**, 021403 (2002).

[100] Chen, S. H., Chen, W. R. & Mallamace, F. The Glass-to-Glass Transition and Its End Point in a Copolymer Micellar System. *Science* **300**, 619–622 (2003).

[101] Bonn, D., Kellay, H., Tanaka, H., Wegdam, G. & Meunier, J. Laponite: What Is the Difference Between a Gel and a Glass? *Langmuir* **15**, 7534–7536 (1999).

[102] Zaccarelli, E. Colloidal Gels: Equilibrium and Non-Equilibrium Routes. *Journal of Physics Condensed Matter* **19**, 323101 (2007).

[103] Zaccarelli, E. & Poon, W. C. K. Colloidal Glasses and Gels: The Interplay of Bonding and Caging. *Proceedings of the National Academy of Sciences* **106**, 15203–15208 (2009).

[104] Kowalczyk, P., Ciach, A., Gauden, P. A. & Terzyk, A. P. Equilibrium Clusters in Concentrated Lysozyme Protein Solutions. *Journal of Colloid and Interface Science* **363**, 579–584 (2011).

[105] Baumketner, A. & Cai, W. Clusters of Lysozyme in Aqueous Solutions. *Physical Review E* **98**, 032419 (2018).

[106] Liu, J., Nguyen, M. D. H., Andya, J. D. & Shire, S. J. Reversible Self-Association Increases the Viscosity of a Concentrated Monoclonal Antibody in Aqueous Solution. *Journal of Pharmaceutical Sciences* **94**, 1928–1940 (2005).

[107] Liu, Y. Colloidal Systems with both a Short-Range Attraction and a Long-Range Repulsion. *Chem Eng Process Tech* **1**, 1010 (2013).

[108] Lindner, P. & Zemb, T. (eds.) *Neutrons, X-Rays and Light: Scattering Methods Applied to Soft Condensed Matter* (Elsevier B.V., Amsterdam, The Netherlands, 2002), first edn.

[109] Wyatt, P. J. Light Scattering and the Absolute Characterization of Macromolecules. *Analytica Chimica Acta* **272**, 1–40 (1993).

[110] Lorber, B., Fischer, F., Bailly, M., Roy, H. & Kern, D. Protein Analysis by Dynamic Light Scattering: Methods and Techniques for Students. *Biochemistry and Molecular Biology Education* **40**, 372–382 (2012).

[111] Hassan, P. A., Rana, S. & Verma, G. Making Sense of Brownian Motion: Colloid Characterization by Dynamic Light Scattering. *Langmuir* **31**, 3–12 (2015).

[112] Koppel, D. E. Analysis of Macromolecular Polydispersity in Intensity Correlation Spectroscopy: The Method of Cumulants. *The Journal of Chemical Physics* **57**, 4814–4820 (1972).

[113] Frisken, B. J. Revisiting the Method of Cumulants for the Analysis of Dynamic Light-Scattering Data. *Applied Optics* **40**, 4087–4091 (2001).

[114] Pusey, P. N. Suppression of Multiple Scattering by Photon Cross-Correlation Techniques. *Current Opinion in Colloid and Interface Science* **4**, 177–185 (1999).

[115] Segrè, P. N., van Megen, W., Pusey, P. N., Schätzel, K. & Peters, W. Two-Colour Dynamic Light Scattering. *Journal of Modern Optics* **42**, 1929–1952 (1995).

[116] Urban, C. & Schurtenberger, P. Characterization of Turbid Colloidal Suspensions Using Light Scattering Techniques Combined with Cross-Correlation Methods. *Journal of Colloid and Interface Science* **207**, 150–158 (1998).

[117] Block, I. D. & Scheffold, F. Modulated 3d Cross-Correlation Light Scattering: Improving Turbid Sample Characterization. *Review of Scientific Instruments* **81**, 123107 (2010).

[118] Waigh, T. A. Microrheology of Complex Fluids. *Reports on Progress in Physics* **68**, 685–742 (2005).

[119] Gardel, M. L., Valentine, M. T. & Weitz, D. A. Microrheology. In Breuer, K. (ed.) *Microscale Diagnostic Techniques*, chap. 1, 1–49 (Springer, 2005).

[120] Cicuta, P. & Donald, A. M. Microrheology: A Review of the Method and Applications. *Soft Matter* **3**, 1449–1455 (2007).

[121] Squires, T. M. & Mason, T. G. Fluid Mechanics of Microrheology. *Annual Review of Fluid Mechanics* **42**, 413–438 (2010).

[122] Mansel, B., Keen, S., Patty, P., Hemar, Y. & Williams, M. A Practical Review of Microrheological Techniques. In Durairaj, R. (ed.) *Rheology New Concepts, Applications and Methods*, chap. 1, 1–22 (Intech, 2013).

[123] Moschakis, T. Microrheology and Particle Tracking in Food Gels and Emulsions. *Current Opinion in Colloid and Interface Science* **18**, 311–323 (2013).

[124] Furst, E. M. & Squires, T. M. *Microrheology* (Oxford University Press, Oxford, UK, 2017), 1st edn.

[125] Zia, R. N. Active and Passive Microrheology: Theory and Simulation. *Annual Review of Fluid Mechanics* **50**, 371–405 (2018).

[126] Mason, T. G. & Weitz, D. A. Optical Measurements of Frequency-Dependent Linear Viscoelastic Moduli of Complex Fluids. *Physical Review Letters* **74**, 1250 (1995).

[127] Mason, T. G., Gang, H. & Weitz, D. A. Rheology of Complex Fluids Measured by Dynamic Light Scattering. *Journal of Molecular Structure* **383**, 81–90 (1996).

[128] Mason, T. G., Gang, H. & Weitz, D. A. Diffusing-wave-spectroscopy Measurements of Viscoelasticity of Complex Fluids. *Journal of the Optical Society of America A* **14**, 139–149 (1997).

[129] Mason, T. G., Ganesan, K., van Zanten, J. H., Wirtz, D. & Kuo, S. C. Particle Tracking Microrheology of Complex Fluids. *Physical Review Letters* **79**, 3282–3285 (1997).

[130] Gittes, F., Schnurr, B., Olmsted, P. D., MacKintosh, F. C. & Schmidt, C. F. Microscopic Viscoelasticity: Shear Moduli of Soft Materials Determined from Thermal Fluctuations. *Physical Review Letters* **79**, 3286–3289 (1997).

[131] Gisler, T. & Weitz, D. A. Tracer Microrheology in Complex Fluids. *Current Opinion in Colloid & Interface Science* **3**, 586–592 (1998).

[132] Mason, T. G. Estimating the Viscoelastic Moduli of Complex Fluids Using the Generalized Stokes-Einstein Equation. *Rheologica Acta* **39**, 371–378 (2000).

[133] Dasgupta, B. R., Tee, S. Y., Crocker, J. C., Frisken, B. J. & Weitz, D. A. Microrheology of Polyethylene Oxide Using Diffusing Wave Spectroscopy and Single Scattering. *Physical Review E* **65**, 051505 (2002).

[134] Breedveld, V. & Pine, D. J. Microrheology as a Tool for High-Throughput Screening. *Journal of Materials Science* **38**, 4461–4470 (2003).

[135] Valentine, M. T., Perlman, Z. E., Gardel, M. L., Shin, J. H., Matsudaira, P., Mitchison, T. J. & Weitz, D. A. Colloid Surface Chemistry Critically Affects Multiple Particle Tracking Measurements of Biomaterials. *Biophysical Journal* **86**, 4004–14 (2004).

[136] Panorchan, P., Wirtz, D. & Tseng, Y. Structure-Function Relationship of Biological Gels Revealed by Multiple-Particle Tracking and Differential Interference

Contrast Microscopy: The Case of Human Lamin Networks. *Physical Review E* **70**, 041906 (2004).

[137] Chae, B. S. & Furst, E. M. Probe Surface Chemistry Dependence and Local Polymer Network Structure in F-Actin Microrheology. *Langmuir* **21**, 3084–3089 (2005).

[138] Tu, R. S. & Breedveld, V. Microrheological Detection of Protein Unfolding. *Physical Review E* **72**, 041914 (2005).

[139] Corrigan, A. M. & Donald, A. M. Particle tracking microrheology of gel-forming amyloid fibril networks. *European Physical Journal E* **28**, 457–462 (2009).

[140] Pan, W., Filobelo, L., Pham, N. D. Q., Galkin, O., Uzunova, V. V. & Vekilov, P. G. Viscoelasticity in Homogeneous Protein Solutions. *Physical Review Letters* **102**, 058101 (2009).

[141] Scherer, T. M., Leung, S., Owyang, L. & Shire, S. J. Issues and Challenges of Subvisible and Submicron Particulate Analysis in Protein Solutions. *The AAPS Journal* **14**, 236–243 (2012).

[142] Josephson, L. L., Furst, E. M. & Galush, W. J. Particle Tracking Microrheology of Protein Solutions. *Journal of Rheology* **60**, 531–540 (2016).

[143] Bauer, K. C., Schermeyer, M.-T., Seidel, J. & Hubbuch, J. Impact of Polymer Surface Characteristics on the Microrheological Measurement Quality of Protein Solutions - A Tracer Particle Screening. *International Journal of Pharmaceutics* **505**, 246–254 (2016).

[144] Garting, T. & Stradner, A. Optical Microrheology of Protein Solutions Using Tailored Nanoparticles. *Small* **14**, 1801548 (2018).

[145] McGrath, J. L., Hartwig, J. H. & Kuo, S. C. The Mechanics of F-Actin Microenvironments Depend on the Chemistry of Probing Surfaces. *Biophysical journal* **79**, 3258–3266 (2000).

[146] Ehrenberg, M. & McGrath, J. L. Binding Between Particles and Proteins in Extracts: Implications for Microrheology and Toxicity. *Acta Biomaterialia* **1**, 305–315 (2005).

[147] Vyas, B. M., Orpe, A. V., Kaushal, M. & Joshi, Y. M. Passive Microrheology in the Effective Time Domain: Analyzing Time Dependent Colloidal Dispersions. *Soft Matter* **12**, 8167–8176 (2016).

[148] Larsen, T. H. & Furst, E. M. Microrheology of the Liquid-solid Transition During Gelation. *Physical Review Letters* **100**, 146001 (2008).

[149] Larsen, T., Schultz, K. & Furst, E. M. Hydrogel Microrheology near the Liquid-Solid Transition. *Korea-Australia Rheology Journal* **20**, 165–173 (2008).

[150] Amin, S., Rega, C. A. & Jankevics, H. Detection of Viscoelasticity in Aggregating Dilute Protein Solutions Through Dynamic Light Scattering-Based Optical Microrheology. *Rheologica Acta* **51**, 329–342 (2012).

[151] Vasbinder, A. J., van Mil, P. J. J. M., Bot, A. & de Kruif, K. G. Acid-Induced Gelation of Heat-treated Milk Studied by Diffusing Wave Spectroscopy. *Colloids and Surfaces B: Biointerfaces* **21**, 245–250 (2001).

[152] Kuimova, M. K., Botchway, S. W., Parker, A. W., Balaz, M., Collins, H. A., Anderson, H. L., Suhling, K. & Ogilby, P. R. Imaging Intracellular Viscosity of a Single Cell During Photoinduced Cell Death. *Nature Chemistry* **1**, 69–73 (2009).

[153] Wirtz, D. Particle-Tracking Microrheology of Living Cells: Principles and Applications. *Annual Review of Biophysics* **38**, 301–326 (2009).

[154] Huang, F., Watson, E., Dempsey, C. & Suh, J. Real-Time Particle Tracking for Studying Intracellular Trafficking of Pharmaceutical Nanocarriers. *Methods in Molecular Biology* **991**, 211–223 (2013).

[155] Zheng, Z., Zou, J., Li, H., Xue, S., Wang, Y. & Le, J. Microrheological Insights into the Dynamics of Amyloplasts in Root Gravity-Sensing Cells. *Molecular Plant* **8**, 660–663 (2015).

[156] Maret, G. Diffusing-Wave Spectroscopy. *Current Opinion in Colloid & Interface Science* **2**, 251–257 (1997).

[157] Scheffold, F., Romer, S., Cardinaux, F., Bissig, H., Stradner, A., Rojas-Ochoa, L. F., Trappe, V., Urban, C., Skipetrov, S. E., Cipelletti, L. & Schurtenberger, P. New Trends in Optical Microrheology of Complex Fluids and Gels. *Trends in Colloid and Interface Science XVI* **123**, 141–146 (2004).

[158] Mason, T. G. New Fundamental Concepts in Emulsion Rheology. *Current Opinion in Colloid & Interface Science* 231–238 (1999).

[159] Corredig, M. & Alexander, M. Food Emulsions Studied by DWS: Recent Advances. *Trends in Food Science & Technology* **19**, 67–75 (2008).

[160] Romer, S., Scheffold, F. & Schurtenberger, P. Sol-Gel Transition of Concentrated Colloidal Suspensions. *Physical Review Letters* **85**, 4980–4983 (2000).

[161] Cloitre, M., Borrega, R., Monti, F. & Leibler, L. Glassy Dynamics and Flow Properties of Soft Colloidal Pastes. *Physical Review Letters* **90**, 068303 (2003).

[162] Hemar, Y., Singh, H. & Horne, D. S. Determination of Early Stages of Rennet-induced Aggregation of Casein Micelles by Diffusing Wave Spectroscopy and Rheological Measurements. *Current Applied Physics* **4**, 362–365 (2004).

[163] Moschakis, T., Murray, B. S. & Dickinson, E. Particle Tracking Using Confocal Microscopy to Probe the Microrheology in a Phase-Separating Emulsion Containing Nonadsorbing Polysaccharide. *Langmuir* **22**, 4710–4719 (2006).

[164] Moschakis, T., Chantzos, N., Biliaderis, C. G. & Dickinson, E. Microrheology and Microstructure of Water-in-Water Emulsions Containing Sodium Caseinate and Locust Bean Gum. *Food & Function* **9**, 2840–2852 (2018).

[165] Savin, T. & Doyle, P. S. Static and Dynamic Errors in Particle Tracking Microrheology. *Biophysical Journal* **88**, 623–638 (2005).

[166] Prasad, V., Semwogerere, D. & Weeks, E. R. Confocal Microscopy of Colloids. *Journal of Physics Condensed Matter* **19**, 113102 (2007).

[167] Jenkins, M. C. & Egelhaaf, S. U. Confocal Microscopy of Colloidal Particles: Towards Reliable, Optimum Coordinates. *Advances in Colloid and Interface Science* **136**, 65–92 (2008).

[168] London, F. The general theory of molecular forces. *Transactions of the Faraday Society* **33**, 8–26 (1937).

[169] Buckingham, A. D., Fowler, P. W. & Hutson, J. M. Theoretical Studies of van der Waals Molecules and Intermolecular Forces. *Chemical Reviews* **88**, 963–988 (1988).

[170] Jenkins, P. & Snowden, M. Depletion Flocculation in Colloidal Dispersions. *Advances in Colloid and Interface Science* **68**, 57–96 (1996).

[171] Poon, W. C. K. The Physics of a Model Colloid-Polymer Mixture. *Journal of Physics Condensed Matter* **14**, R859–R880 (2002).

[172] Tuinier, R., Rieger, J. & de Kruif, C. G. Depletion-Induced Phase Separation in Colloid-Polymer Mixtures. *Advances in Colloid and Interface Science* **103**, 1–31 (2003).

[173] Lekkerkerker, H. N. W. and Tuinier, R. *Colloids and the Depletion Interaction* (Springer, Heidelberg, Germany, 2011).

[174] Tuinier, R., Fan, T.-H. H. & Taniguchi, T. Depletion and the Dynamics in Colloid-Polymer Mixtures. *Current Opinion in Colloid and Interface Science* **20**, 66–70 (2015).

[175] Valeur, E. & Bradley, M. Amide bond formation: Beyond the myth of coupling reagents. *Chemical Society Reviews* **38**, 606–631 (2009).

[176] Vashist, S. K. Comparison of 1-Ethyl-3-(3-Dimethylaminopropyl) Carbodiimide Based Strategies to Crosslink Antibodies on Amine-Functionalized Platforms for Immunodiagnostic Applications. *Diagnostics* **2**, 23–33 (2012).

[177] Dawson, R. M. C., Elliot, D. C., Elliot, W. H. & Jones, K. M. (eds.) *Data for Biochemical Research* (Oxford Press, Oxford, 1987), 3 edn.

[178] Bhattacharjee, S. DLS and Zeta Potential - What They Are and What They Are Not? *Journal of Controlled Release* **235**, 337–351 (2016).

[179] Larsson, M., Rega, C. A., Duffy, J. & Jankevics, H. Detection of Viscoelasticity in Aggregating Dilute Protein Solutions through Dynamic Light Scattering-Based Optical Microrheology. *Annual Transactions of the Nordic Rheology Society* **20**, 183–200 (2012).

[180] Crocker, J. C. & Grier, D. G. Methods of Digital Video Microscopy for Colloidal Studies. *Journal of Colloid and Interface Science* **179**, 298–310 (1996).

[181] Valentine, M. T., Kaplan, P. D., Thota, D., Crocker, J. C., Gisler, T., Prud'homme, R. K., Beck, M. & Weitz, D. A. Investigating the Microenvironments of Inhomogeneous Soft Materials with Multiple Particle Tracking. *Physical Review E* **64**, 061506 (2001).

[182] Zakharov, P. Mie Calculator; https://www.lsinstruments.ch/mie_calculator/; Accessed: 2017-01-17 (2004).

[183] Gombotz, W. R., Guanghui, W., Horbett, T. A. & Hoffman, A. S. Protein Adsorption to Poly(Ethylene Oxide) Surfaces. *Journal of Biomedical Materials Research* **25**, 1547–1562 (1991).

[184] Gombotz, W. R., Guanghui, W., Horbett, T. A. & Hoffman, A. S. Protein Adsorption to and Elution from Polyether Surfaces. In Harris, J. M. (ed.) *Poly(Ethylene Glycol) Chemistry Biotechnical and Biomedical Applications*, chap. 16 (Springer Science+Business Media, LLC, New York, 1992), first edit edn.

[185] Holmberg, K. & Harris, J. M. Poly(Etheylene Glycol) Grafting as a Way to Prevent Protein Adsorption and Bacterial Adherence. In van Ooij, W. J. & Anderson Jr, H. R. (eds.) *First International Congress on Adhesion Science and Technology - Invited Papers*, 443–461 (CRC Press, Utrecht, 1998), 1 edn.

[186] Feigin, R. I. & Napper, D. H. Stabilization of Colloids by Free Polymer. *Journal of Colloid And Interface Science* **74**, 567–571 (1980).

[187] Feigin, R. I. & Napper, D. H. Depletion Stabilization and Depletion Flocculation. *Journal of Colloid And Interface Science* **75**, 525–541 (1980).

[188] Bonn, D., Otwinowski, J., Sacanna, S., Guo, H., Wegdam, G. & Schall, P. Direct Observation of Colloidal Aggregation by Critical Casimir Forces. *Physical Review Letters* **103**, 156101 (2009).